Advances in Materials Research, *Vol. 14, No. 2 (2025) 125-162*
https://doi.org/10.12989/amr.2025.14.2.125

Enhancing lightweight concrete with silica fume: A nonlinear finite element analysis of plastic damage

Lamiaa K. Idriss*[1] and Yasser A.S Gamal[2,3]

[1]*Department of Civil Engineering, Sphinx university, Assiut, Egypt*
[2]*Department of Civil Engineering, High Institute of Engineering Technology, EL-MINA, Egypt*
[3]*Department of Civil Engineering, Faculty of Engineering, NUB university, Egypt*

(*Received October 4, 2024, Revised February 17, 2025, Accepted April 11, 2025*)

Abstract. The paper presents a novel plastic-damage constitutive model for two types of lightweight concrete (LWC), namely aerated concrete (AC) and recycled coarse concrete with no fine aggregate (RC). The model has the potential to improve the ductility and toughness of the LWC, while simultaneously reducing its damage level. The amount of silica fume (SF) used in the concrete mix determines the extent of these improvements. Therefore, an experimental investigation was used to determine the optimal percentage of (SF) that should be used in the proposed model for the two types (LWC). These types of concrete included recycled coarse aggregate at a ratio of 6:1 to the amount of cement, which allowed for the incorporation of waste materials into the concrete mix. Additionally, aerated concrete (AC) was produced by adding composite fly ash (FA) and aluminum powder (AL) in proportions of 10% and 0.2%, respectively, based on the weight of the cement fresh and hardened concrete tests were carried out, for 7,14, and 28 days on the samples tested consisted of 36 cubes measuring 150 x 150 x 150 mm and 9 cylinders measuring 150 mm in diameter and 300 mm in height, the highest compressive strength was achieved when using an optimal proportion of SF and FA in AC3 and RC3 for aerated and recycled (LWC), respectively. This proportion involved a 20% addition of silica fume (based on cement content). Furthermore, the numerical study demonstrated that the proposed algorithm is effective and resilient in finite element analysis FEA ABAQUS software to develop a concrete plastic-damage (CDP) constitutive model suitable for RC3 and AC3 to simulate the tension stiffening behavior with stress strain diagram. This model employs two damage variables to represent tensile and compressive damage independently. Furthermore, this model utilizes a combined approach of continuum damage mechanics and plasticity theory, which is known as the compression cylinder model of lightweight concrete with a damage plasticity (CDP) method. These investigations also provide valuable insights into the impact of SF on the plasticity behavior of LWC concrete, which can enhance its ductility, and toughness, and reduce its damage level depending on the percentage of SF. In addition, the numerical results employ statistical regression analysis to establish the equations that indicate the relationship between compression stress and tensile strength (fc and ft) for high-strength values from all samples (AC3 and RC3).

Keywords: ABAQUS /CAE; aerated concrete; lightweight concrete; no fine concrete; silica fume; plastic concrete damage; stress-strain relations

1. Introduction

*Corresponding author, Associate professor.,
E-mail: Yasser.gamal2310@mhiet.edu.eg; yasser.abdelshafy@nub.edu.eg

http://www.techno-press.org/?journal=amr&subpage=5 ISSN: 2234-0912 (Print), 2234-179X (Online)

Lightweight concrete can significantly reduce the dead weight load of a structure. Meanwhile, self-compacting concrete simplifies the pouring process and eliminates construction issues associated with vibration and compaction. Combining the benefits of lightweight and self-compacting concrete presents an innovative area for research. Given its ability to both lighten the structure and streamline placement, self-compacting lightweight concrete shows promise as a solution to meet growing construction demands for slimmer, more densely reinforced structural components. With self-compacting lightweight concrete, structures may realize reduced mass without compromising the ease of installation (Vakhshouri and Nejadi 2016). However, (Chen *et al*. 2011) conducted research on the development of lightweight aggregate concrete (LWC) using fine sediments obtained from the Shihmen Reservoir in Taiwan. The sediments were expanded using high heat to create the lightweight aggregate. The study aimed to evaluate the performance of the concrete and prestressed concrete beams made from the sedimentary LWA, comparing them with beams made from normal-weight concrete (NC). The test results revealed that the lightweight concrete (LWC) exhibited similar time-dependent properties, such as compressive strength, elastic modulus, drying shrinkage, and creep, when compared to the NC samples. Furthermore, the LWC beams demonstrated a lower percentage of prestress loss compared to the NC beams. On average, the LWC beams could sustain loads up to 96% of the NC beams' capacity, and the experimental strengths surpassed the nominal strengths calculated using the ACI Code method.

However, construction and demolition (C&D) waste can be recycled and repurposed as a raw material for producing new recyclable aggregates. The process involves crushing and sorting the waste into different categories based on the type of material. The sorted materials are then crushed and sieved to produce different sizes of recycled aggregate, which can be used in various applications such as road construction, embankments, and construction building (Batayneh *et al*. 2007, Joohari *et al*. 2018).

The analysis of plasticity damage in lightweight concrete examines how the material responds to loading and deformation conditions. When subjected to excessive stress or strain, the material experiences permanent deformation and reduced load-carrying capacity (Chen *et al*. 2007, Jankowiak and Lodygowski 2005). Lightweight concrete's unique composition, featuring lightweight aggregates and air voids, results in distinct behavioral characteristics compared to conventional concrete, particularly in terms of strength, stiffness, and durability. The modeling approach commonly employed for lightweight concrete incorporates both plastic components based on effective stress and damage components based on total strain deformation measures, facilitating an efficient coupling of plasticity and damage mechanisms (Yu *et al*. 2010).

The study investigated lightweight concrete (LWC) performance by examining two distinct types: aerated concrete (AC) incorporating silica fume (SF) (at 10%, 15%, and 20% of cement weight) along with fly ash (FA) (0.2%) and aluminum powder (AL) (10%), and reinforced concrete without fine aggregates. The research methodology included comprehensive testing of fresh concrete properties (slump, compaction factor, density, porosity, void ratio, and water absorption) and strength characteristics (splitting tensile and compressive strength) at 7, 14, and 28-day intervals. Through extensive finite element analysis using ABAQUS software, the study evaluated the concrete damage plasticity (CDP) model's effectiveness, particularly focusing on the comparative analysis of stress-strain behavior between AC3 (aerated concrete) and RC3 (reinforced concrete).

2. Literature review

Lightweight aggregates are an essential component in the construction industry, offering a range

of benefits over conventional aggregates. And, the two primary types of lightweight aggregate are natural and artificial, each with its unique characteristics and applications. Natural lightweight aggregates are formed from natural materials such as volcanic pumice, clay, shale, and slate. These aggregates are characterized by their low density, high porosity, and good insulation properties, making them ideal for use in concrete, lightweight blocks, and precast panels.

The study of lightweight aggregates has been conducted worldwide due to their potential benefits. However, concrete made with these lightweight aggregates typically has lower compressive strength. On the other hand, research has indicated that lightweight concrete blocks that have been damaged can be easily recycled and used as lightweight aggregates in the production of geopolymer blocks with adequate strength and density (Posi *et al*. 2016). As a result, numerous researchers have directed their efforts towards the study of lightweight concrete in order to improve its performance characteristics. By focusing their work on understanding and enhancing the behavior of lightweight concrete, these researchers aim to advance the material's properties and potentially expand its applications in construction. Their goal is to develop lightweight concrete that exhibits enhanced behaviors over previous versions of the material.

Behnam Vakhshouri (2020) examined the properties of lightweight concrete containing expanded polystyrene beads (EPS-LWC). EPS-LWC has been approved for use in structural and non-structural applications. Compared to concrete made with ordinary aggregates, EPS-LWC has a considerably lower density and higher structural efficiency. Vakhshouri's experimental testing generated new data on the mechanical properties of structural EPS-LWC. This includes information on strength under tension (from splitting and bending tests), modulus of elasticity, unconfined compressive stress-strain behavior, energy absorption under compression, and reinforcement-concrete bond characteristics. The study provides valuable insights into the performance of this lightweight concrete material.

Majhi focused on developing sustainable structural lightweight concrete (LWC) by incorporating a significant amount of fly ash chemosphere (FAC) as a replacement for natural fine aggregate (NFA). Additionally, silica fume (SF) was used as a substitute for ordinary Portland cement (OPC) to enhance the concrete mix. Various concrete mixes were designed with different combinations of FAC (60%, 80%, and 100%), SF (10%, 15%, and 20%), and water-binder (W/B) ratios (0.40, 0.44, and 0.48) (Majhi *et al*. 2021). The mechanical and physical properties of these mixes were then evaluated. The experimental results indicate that the appropriate dosage of SF improves the properties of high-volume FAC-based concrete. As a result, the structural LWC produced meets the strength and density criteria outlined in the ACI 213R-14 guidelines (INSTITUTE 2014). In addition, foam concrete containing silica fume demonstrated superior heat resistance when subjected to 1200°C temperatures, with permeability values of 6.5% and 5.3% - showing better performance than control samples. The addition of silica fume enhanced both the long-term compressive strength and thermal insulation characteristics of the foam concrete material (Şeker *et al*. 2022).

In addition, Fahmy and Idriss had an objective in their study to examine the flexural behavior of T-section semi-precast reinforced concrete (RC) beams constructed using recycled aggregate concrete (RAC) and natural aggregate concrete (NC). The experimental program included four large-scale T beams. Furthermore, the study explored the potential of utilizing precast RAC blocks as fillers in the web core of RC beams. This construction technique shows promise and can serve as a crucial design parameter for effectively managing the development, propagation, and width of flexural and shear cracks in a significant manner (Fahmy and Idriss 2019).

Kalyana studied fracture mechanics, which has gained importance for understanding crack behavior. The study evaluated the fracture energy and characteristic length for different grades of

concrete using the Concrete Damage Plasticity (CDP) model in the Finite Element Analysis software ABAQUS/CAE. The results indicated that the CDP model can accurately predict the fracture properties of concrete for various grades without laboratory testing. Generally, improper mix design, poor curing conditions, and exposure to harsh environments can lead to plastic damage in lightweight concrete. Proper mix design, adequate curing, and appropriate reinforcement are key to minimizing plastic damage in lightweight concrete (Kalyana Rama *et al*. 2017).

Parande emphasized that the demand for high compressive strength in concrete specifications should be justified by specific design advantages. High-Performance Concrete (HPC) utilizes blended cements that incorporates materials like silica fume, fly ash, and ground granulated blast-furnace slag. These cementitious materials can constitute more than 25% of the total cement weight in typical formulations. Silica fume contributes to strength and durability, while fly ash and slag cement enhance finish quality, reduce permeability, and increase resistance to chemical attack. The study discusses the effects of various mineral admixtures, such as fly ash, silica fume, micro silica, and slag, on the performance of high-strength concrete (Parande 2013). Furthermore, Verma focused on developing recycled concrete aggregate (RCA) as an alternative to natural resources, which are being depleted rapidly due to the increasing demand of the concrete industry. The use of RCA in landfills and concrete manufacturing can help mitigate this issue. RCA utilization offers cost savings and improved energy utilization. The study presented the mechanical behavior of concrete containing successively recycled concrete aggregate (RCA). In the mix design, RCA was used as a complete replacement for natural aggregates (NA). The test results for compressive strength, flexural strength, and pulse velocity were obtained at curing ages of 14 and 28 days, demonstrating significant improvements compared to conventional concrete (Verma and Ashish 2017).

Haido studied the behavior of concrete incorporating waste glass as a replacement for cement or aggregate. However, this investigation focuses on the recycling of waste glass powder as a substitute for silica fume in high-strength concrete (HSC). The study utilized the same constitutive relationships to model the behavior of HSC, comparing the performance of beams made with waste glass powder and silica fume. The findings of the study indicated that HSC beams incorporating waste glass powder exhibited enhanced ultimate load-carrying capacity and ductility compared to HSC specimens containing silica fume. This suggests that the use of waste glass powder as a substitute for silica fume in HSC can lead to improved performance in terms of both load-bearing capacity and ductility (Haido *et al*. 2021).

Osama *et al*. (2023) examined eco-friendly concrete (Eco-Con) reinforced slabs through two types of tests. The first evaluated how two-way slabs performed under punching shear conditions, while the second assessed Eco-Con's effectiveness as a repair material for one-way slabs subjected to 4-point bending tests. Results showed that when using Eco-Con rubber engineered cementitious composite, the slab's strength decreased slightly (7%), but its ability to deflect improved by 20% compared to traditional Portland cement concrete slabs. When testing slabs repaired with either geopolymer rubber or geopolymer lightweight expanded clay aggregate mixtures, the bending strength and maximum deflection were similar to those of the cementitious composite slab (Youssf *et al*. 2023).

Abdeliazim *et al.* (2023) explored the use of steel fibers in lightweight concrete to develop more sustainable concrete solutions. According to their findings, optimal mechanical properties were observed when steel fiber content was between 0.75% and 1% of the mixture. The addition of steel fibers enhanced the concrete's performance by creating a binding effect that helped distribute shear stresses and reduce crack propagation, ultimately leading to improved structural durability and load-bearing capacity (Mohamed *et al*. 2023).

Mohamed *et al.* (2020) examined how the addition of polypropylene fibers (PPF) and glass fibers (GF) affected lightweight concrete's (LWC) performance, particularly its mechanical properties and behavior at high temperatures. This research demonstrated that incorporating 0.4% glass fibers led to significant improvements, with flexural strength increasing by 53% and tensile strength by 38%. When exposed to high temperatures, concrete containing glass fibers showed enhanced compressive and flexural strength. However, the addition of polypropylene fibers had different effects - it increased concrete porosity, and when subjected to elevated temperatures, the melting of these fibers created air voids and multiple cracks, resulting in substantial decreases in both compressive and flexural strength (Amin and Tayeh 2020).

Bassam *et al.* (2021) investigated how elevated temperatures affect two types of lightweight concrete: geopolymer (LWGC) and ordinary (LWOC). Both varieties were manufactured using natural pumice and lightweight expanded clay aggregate (LECA), with additional air entrainment. The investigation revealed that LWGC achieved peak compressive strength when formulated with equal proportions 50% of fly ash and 50% ground blast furnace slag (GBFS). When subjected to various experimental conditions, both LWGC and LWOC demonstrated comparable behavioral patterns and responses (Tayeh *et al*. 2021).

Bassam *et al.* (2022) conducted exploring the potential use of ferrosilicon slag powder (FSS), a waste product from industry, as an air-entraining agent. The research utilized class F fly ash for geopolymer concrete production and compared the effectiveness of FSS against aluminum powder (AP) as air-entraining agents in lightweight geopolymer concrete. FSS demonstrated superior performance in terms of concrete workability and density compared to AP when used in equal proportions. Testing revealed that concrete containing 1% AP achieved a slump flow of 548mm, density of 1830 kg/m^3, and compressive strength of 24.7 MPa, while concrete with 1% FSS showed values of 569mm, 1740 kg/m^3, and 21.8 MPa respectively (Tayeh *et al*. 2022).

Hussein *et al.* (2022) examined how incorporating nano-sized palm oil fuel ash (POFA) could improve the properties of lightweight concrete made with palm oil clinker (POC) aggregates. Their experimental findings demonstrated that while POC aggregates generally reduced concrete performance metrics, the addition of nano-POFA had an interactive effect on key properties including ultrasonic pulse velocity measurements, flexural strength, and tensile strength. The beneficial impact of nano-POFA became particularly evident in later-age testing, helping to counteract some of the limitations associated with POC aggregate use (Hamada *et al*. 2022).

Yasser *et al.* (2020) explored creating sustainable structural lightweight concrete (SLWC) by completely replacing conventional aggregates with recycled crushed brick waste. The researchers evaluated various cement substitutes, including silica fume, fly ash, metakaolin, and slag, at replacement levels of 5%, 10%, and 15% by cement weight. Their findings revealed that viable SLWC could be produced using 100% waste crushed bricks as aggregate, combined with either 15% metakaolin or 15% silica fume as cement replacements. These mixes achieved notable compressive strengths of 39.5 MPa and 41.5 MPa respectively (Hussein *et al*. 2022).

Ibrahim *et al.* (2020) examined how incorporating agricultural waste products - specifically rice straw ash (RSA) and cotton stalk ash (CSA) affected the performance and internal structure of lightweight self-compacting concrete (LWSCC) when used to partially replace cement. Their experimental investigation revealed that while increasing the proportion of both RSA and CSA reduced workability, it generally enhanced the concrete's hardened properties, though this benefit did not extend to 20% replacement levels. Microstructural analysis through scanning electron microscopy demonstrated that concrete containing 10% RSA achieved greater density compared to specimens without ash additives (Agwa *et al*. 2020).

Hamada *et al.* (2021) investigated the effects of varying amounts of nano-palm oil clinker powder (NPOCP) as a cement substitute in concrete mixtures that used palm oil clinker (POC) as the sole coarse aggregate. The research revealed that higher NPOCP content led to increased workability in the resulting semi-lightweight aggregate concrete (semi-LWAC), while simultaneously reducing the concrete's density. The strength testing demonstrated that replacing 10% of cement with NPOCP produced the best results, achieving a compressive strength of 39 MPa, while a 40% replacement level yielded the lowest strength values among all test specimens (Hamada *et al.* 2021).

Citek *et al.* (2018) examined how heat moves through eco-friendly lightweight concrete that uses recycled polypropylene waste to partially replace traditional aggregates. The results indicated that this lightweight concrete variant showed promise as a building material with enhanced insulation capabilities. Additionally, incorporating recycled plastic waste into the concrete mixture proved advantageous both environmentally and economically (Citek *et al.* 2018).

Taher *et al.* (2021) investigated how adding microscopic cement-based materials affects both the strength characteristics and sulfate resistance in a specially formulated environmentally-friendly lightweight concrete blend. This innovative concrete mixture combined expanded clay aggregate (LECA) with standard crushed dolomite. Testing revealed that incorporating micro-cementitious materials improved the concrete's overall performance. The research notably found that specimens containing micro silica fume demonstrated superior results compared to those with metakaolin. (Taher *et al.* 2021)

Omar *et al.* (2020) explored using two alternative materials in mortar: lightweight fine aggregate (LWFA) and micro rubber ash (MRA) derived from used tires, both serving as sand substitutes. they conducted comprehensive testing on the resulting lightweight rubberized mortar (LWRM), examining various properties including its workability, density, resistance to compression and tension, heat transfer capabilities, shrinkage behavior during drying, and microscopic structure. Testing revealed significant strength reductions when high levels of LWFA were incorporated - specifically, samples containing 75% LWFA exhibited a 64% decrease in compressive strength and a 57% reduction in tensile strength compared to standard mortar mixtures (Ibrahim and Tayeh 2020).

On the other hand, the green recycled aggregate concrete (GRAC) reveals that density significantly affects concrete strength, with higher-density materials producing stronger concrete due to reduced void content. While decreased density improved workability by one-third, material choice greatly influenced performance. The use of crushed waste red brick (CWRB) as fine aggregate and crushed waste cement block (CWCB) as coarse aggregate enhanced compressive strength through better cement paste bonding. Conversely, adding crushed waste plastic bottles (CWPB) diminished both density and bond strength, particularly at 20% plastic content, due to the irregular and angular particle shapes that impeded material flow and compromised structural integrity (Owais and Idriss 2024). In addition, Lamia conducted experimental studies to investigate how different cement varieties influenced the characteristics of concrete containing recycle waste rubber tires (WRT), where the WRT was substituted for recycled coarse aggregates (RCA) at varying (Idriss and Gamal 2022).

On the other hand, artificial lightweight aggregates are produced by heating and expanding clay, shale, or slate in a rotary kiln, resulting in expanded clay, shale, and slate aggregates. These aggregates have a high strength-to-weight ratio, making them suitable for use in structural concrete, lightweight masonry, and bridge decks. The use of lightweight aggregates in construction offers several benefits, including reduced dead load, improved thermal insulation, and increased seismic resistance (Gamal and Abd Elrazek 2022). Additionally, lightweight aggregates can lead to a reduction in transportation costs and environmental impact due to their lower weight and energy

requirements during production. Overall, the use of natural and artificial lightweight aggregates has become increasingly popular in the construction industry due to their numerous advantages and versatility. If there is a need to enhance a building's overall seismic resistance, it is common to replace the gravel with lightweight aggregate, which reduces the structure's deadweight. In these circumstances, it is evident that effective techniques are necessary to enhance the thermal insulation capabilities of single-layer structures by using lightweight aggregate (Hilal *et al*. 2016). On the other hand, the primary determinant of foam concrete's compressive strength and elastic modulus is its internal air void distribution (Kim *et al*. 2012). Modifications to this void network can substantially impact both the microscopic and macroscopic structure of foam concrete, leading to considerable changes in its mechanical behavior (Wee *et al*. 2006).

It is worth highlighting that the lightweight concrete industry has been established with a focus on the primary production of single-layered wall panels. Hence, augmenting the content of lightweight aggregate can decrease the density and thermal conductivity of lightweight concrete. Since concrete constitutes a significant proportion of a structure's total load, decreasing the concrete's dead weight can lead to a reduction in the cross-sectional area of structural components and steel reinforcement. In other words, reducing the density of concrete has evident advantages.

Lightweight concrete (LWC) finds wide-ranging applications, from insulation to structural purposes. No-fine concrete is typically used for external load-bearing and non-load-bearing walls and partitions, as well as infilling panels in framed structures. The second type, lightweight Aggregate Concrete (LWC), offers a lower density and higher thermal insulation capacity than conventional weight aggregate concrete (NWC), leading to its increased and diversified usage across various fields (Yun *et al*. 2013). Furthermore, the strength of LWC is mostly supported by the mortar phase, which contains cement, water, and sand, while the density of LWC is primarily reduced by the LWA phase (Domagala 2020).

Numerous studies have been conducted to examine the impact of aluminum (Al) concentration on the compressive strength of aerated concrete, as reported by (Guglielmi *et al*. 2010). Additionally (Amran *et al*. 2015) explored the performance of different types of blocks and bricks, including aerated concrete, solid and hollow block, and molded wire-cut brick. Nowadays, utilizing concrete with lightweight aggregates (LWA) made from solid waste or recycled by-products (LWRA) is a popular topic in the construction and building materials industry. This approach offers significant advantages in terms of reducing the use of natural resources and minimizing the negative impact on the environment during the production of Portland cement, as highlighted by (Wang *et al*. 2020).

Kabir examined the flexural behavior of slender High Strength Steel (HSS) composite beams that were encased with Engineered Cementitious Composites and Lightweight Concrete (ECC-LWC). The researchers conducted tests on four simply supported slender HSS composite beams, each with different encasement materials (concrete or ECC-LWC) and configurations (fully or partially encased), using a four-point bending setup. The results of the experiments revealed that the two ECC-LWC fully encased slender beams exhibited higher load-carrying capacity and improved ductility compared to the fully encased slender beam made of concrete. However, the partially encased beam, where the encasement was applied only to the compression flange, experienced failure due to lateral torsional buckling before the top flange reached its yielding point (Kabir, Lee *et al*. 2020).

In a recent 2023 study conducted by Nukah, a novel lightweight concrete containing Lytag and silica fume (LSFC) was introduced as a viable option for construction and structural applications. The focus was on evaluating the compressive strength development and stress-strain relationships of LSFC to understand its strength growth and develop a design equation for beams. Comparisons were made between the analysis and design results of LSFC and normal weight concrete (NWC).

The findings revealed that LSFC significantly reduced the required reinforcement by 47% while also exhibiting an increased shear resistance. Furthermore, the stress-strain behavior of LSFC did not show strain softening, indicating favorable flexural strength. Overall, the study demonstrated that LSFC has potential benefits in terms of lowered reinforcement needs, enhanced shear resistance, and preferable stress-strain behavior, making it a promising choice for structural uses (Nukah, Abbey *et al*. 2023).

Plastic damage in lightweight concrete refers to the deformation and failure of the material when it is subjected to loads beyond its elastic limit. In lightweight concrete, the presence of voids and pores can reduce its strength and stiffness, making it more susceptible to plastic damage. The use of lightweight aggregates, such as expanded polystyrene beads or pumice, can also contribute to plastic damage in lightweight concrete due to their lower strength and stiffness compared to traditional aggregates. Other factors that can lead to plastic damage in lightweight concrete include improper mix design, poor curing conditions, and exposure to harsh environmental conditions. And, the proper mix design, adequate curing, and appropriate reinforcement are essential to minimizing plastic damage in lightweight concrete.

The research evaluated two types of lightweight concrete – first type recycle coarse aggregate without sand and the second type is an aerated concrete - focusing on concrete damage plasticity parameters. The study examined how different proportions of silica fume, fly ash, and aluminum powder affect mechanical properties through comprehensive testing of fresh concrete properties and strength characteristics. Using ABAQUS software and statistical regression analysis, the research modeled concrete behavior and established relationships between compression stress and tensile strength, implementing a plastic-damage model to analyze the effects of different material compositions on lightweight concrete performance under loading conditions.

3. Materials and experimental

Two types of lightweight concrete (LWC) were produced in this study. The first type was (RC), which was made using recycled coarse aggregate at a ratio of 6:1 with cement and without fine aggregate. The second type was (AC), which was produced by using composite (FA) and aluminum powder (AL) at 10% and 0.2% by cement weight, respectively. For both types, (SF) was added at 10%, 15%, and 20% by cement weight. The experiment utilized the following material characteristics to create concrete mixes.

The research methodology is illustrated in Fig. 1, outlining the objectives of the study, which include analyzing the impact of silica fume (SF) on improving the properties of lightweight concrete and developing a nonlinear finite element plastic damage model for both aerated and recycled concrete. The figure serves as a roadmap, highlighting the steps required to achieve the research objectives.

The assessment of concrete workability across various consistency levels (low, medium, and high) is conducted using compacting factor equipment alongside standard slump testing apparatus. The slump measurement system consists of a mild steel conical mold with integrated handles and includes a chrome-plated steel rod measuring 16 mm in diameter and 600 mm in length for compaction purposes. The measured slump value serves as an indicator of fresh concrete's consistency and workability characteristics prior to setting. The concrete's air content is evaluated using a Type B pressure meter in accordance with ASTM C231(Astm 2004) specifications, as excessive air void content can significantly compromise the concrete's long-term durability performance.

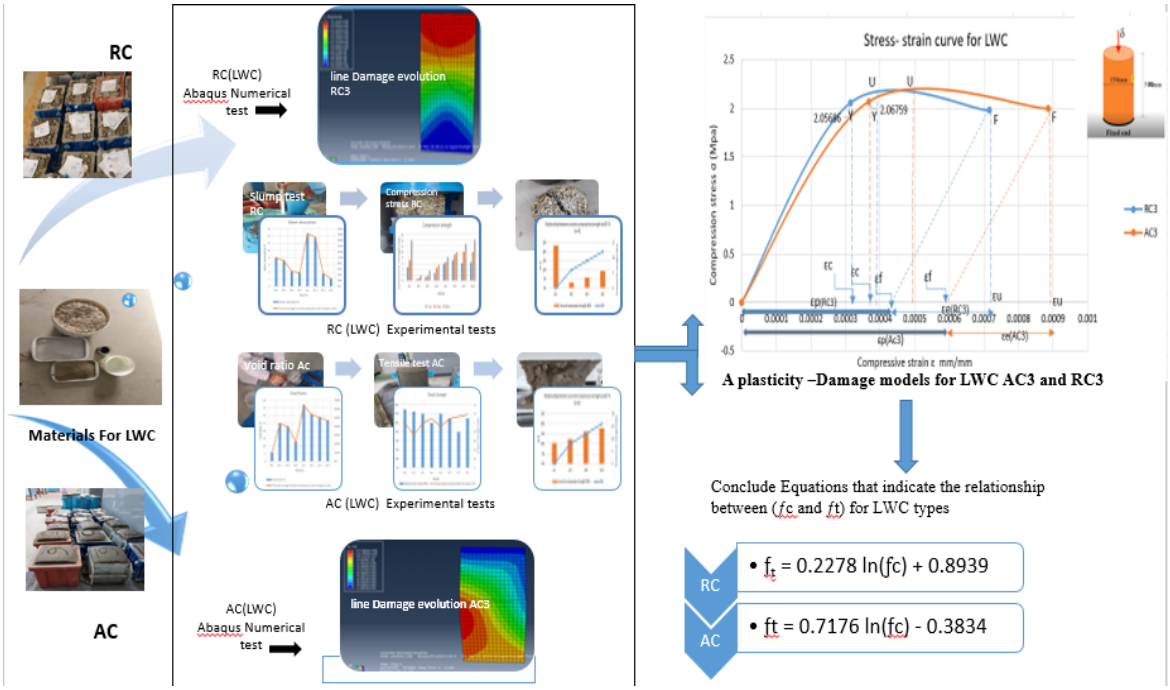

Fig. 1 The road map of research

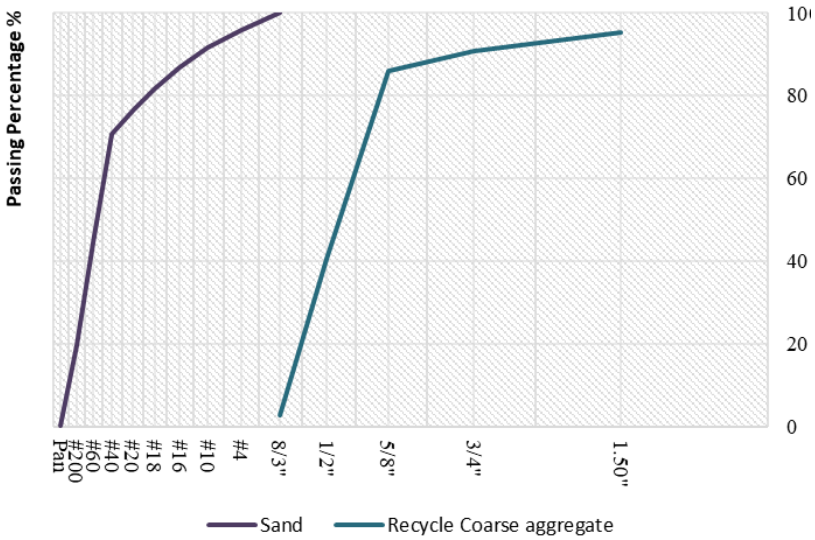

Fig. 2 Aggregate sieve analysis according to ASTM C136

3.1 Aggregate:

To conduct the experiment, specific recycled coarse aggregates and fine sand were utilized, each with distinct properties. The recycled coarse aggregate (RCA) was sourced from a multitude of pretested concrete cubes obtained from construction companies in Egypt. The RCA was then crushed


(a) Recycled concrete cubic


(b) Specific gravity gravel


(c) Crushing value

Fig. 3 Recycle coarse aggregate tests [RCA]


(a) Void ratio


(b) Specific gravity

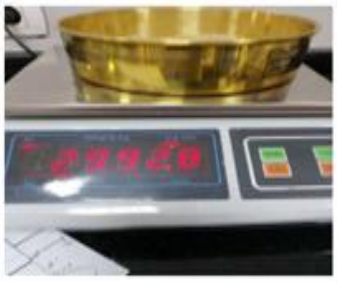
(c) Sieves Analysis

Fig. 4 Fine aggregate tests

Table 1 Physical properties of recycle coarse aggregates (RCA)

Properties	Test results value	Egyptian Standard
Specific gravity	2650kg/m^3	---
Bulk density of RCA	1250kg/m^3	----
Water absorption (%)	3.06%	---
Void ratio (%)	52.53%	----
Crushing value (%)	21.80%	Not more than 25%
Total porosity %	20%	----
Fineness modulus	725018.22kg/m^2	Max. size of RCA 40mm

Table 2 Sieve Analysis for (RCA)

Sieve No	Diameter (mm)	Mass of sieve (g)	Mass full of sieve	Mass retained	Cumulative weight	Cumulative percentage	% of passing
1.50”	40	1007	1100	93	93	4.65	95.35
3/4”	20.00	1007	1100	93	186	9.3	90.7
5/8”	16.00	1007	1100	93	279	14.0	86.05
1/2”	12.50	1007	1919	912	1191	59.6	40.45
8/3”	10.000	1010	1765	755	1946	97.3	2.7
#4	4.750	1046	1100	54	2000	100.0	0
#10	2.36	828	828	0.0	2000	100.0	0
Total					2000		

Table 3 Physical properties of fine aggregate(sand)

Properties	Test results value
Specific gravity	2650Kg/m^3
bulk density of Sand	1250kg/m^3
Fineness modulus	312033.16kg/m^2
Void ratio (%)	52.53%

Table 4 Sieve analysis of fine aggregate [sand]

Sieve No	Diameter (mm)	Mass of sieve (g)	Mass full of sieve	Mass retained	Cumulative weight	Cumulative percentage	% of passing
	10	1050	1050	0	0	0	100
#4	4.75	1046	1127	81	81	4.1	95.94
#10	2.36	828	913	85	166	8.3	91.69
#16	2	808	902	94	260	13	86.99
#18	1.7	1127	1230	103	363	18.2	81.84
#20	1.18	754	860	106	469	23.50	76.54
#40	0.8	658	775	117	586	29.3	70.69
#60	0.3	660	1186	526	1112	55.6	44.39
#200	0.15	660	1152	492	1604	80.2	19.79
Pan	0.08	660	1050	390	1994	99.7	0.296
		374.07	350	5.9	1999.9	100	

Table 5 Physical and mechanical properties of cement (OPC) CEM 11/B-P (32.50 N)

Properties	Test results value	(ES4756-1 / 2009)
% of water for standard consistency	33.3%	
Specific surface area (Bline)m^2/kg	2827 m^2/kg	Not less than 2750
Specific gravity	3150Kg/m^3	
bulk density of cement	1140 Kg/m^3	
Soundness (Le chatelier)	7.50mm	Not more than 10mm
Initial setting-time (min)	200	Not less than 45 min
Final setting time (min)	420	Not more than 10 hr.
Compressive strength of standard mortar		
3days (MPa)	14.5	Not less than 32.5
27 days (MPa)	34	

to a size of 20mm and tested according to the ES:1109/2002 standards prior to use in the experiment. Similarly, the siliceous sand was also tested according to ES:1109/2002 standards (1109/2002 2002).

The properties and sieve analysis of the recycled coarse aggregate are detailed in Tables 1, 2, while Tables 3 and 4 present the properties and sieve analysis of the fine sand. The passing percentage for both types of aggregates is depicted in Fig. 2, while Figs. 3 and 4 illustrate the tests carried out on the recycled coarse and fine aggregates, respectively.

Table 6 Physical and Mechanical Properties of superplasticizer Sikament 163 M(SP)

Properties	Test results value
PH value	4.3–4.7
Density at 20°C	1.20 kg/liter
Fineness modulus	312033.16117kg/m^2
Void ratio (%)	52.53%

Table 7 Physical and Mechanical Properties of Silica Fume [Sika data sheet] (SF)

Specific Gravity	2150kg/m^3
Mean grain size	7
Specific surface area(m^2/kg)	178000
Bulk density (Kg/m^3)	3450
Silicon dioxide SiO_2	96
Aluminum oxide AL_2O_3	1.1
Calcium oxide CaO	1.2
Magnesium Oxide MgO	0.18
Potassium oxide K_2O	1.2
Sodium oxide Na_2O	0.45
Sulfur dioxide SO_2	0.45
Water H_2O	0.85
color	Light Gray

3.2 Cement (OPC):

Table 5 presents the chemical and physical properties of the ordinary Portland cement [CEM 11/B-P] utilized in the studies, and it had been tested according to (ES:4756- 1/2009) (E.S.S.4756-1/2009 2009).

3.3 Sikament-163M (SP):

Sikament-163 M, a superplasticizer manufactured by Sika Egypt, was used in the experiment to accelerate both the early and ultimate strength gains of the concrete. And, it conforms to the A.S.T.M. C 494-92 Type F standard. Sikament-163 M was among the superplasticizers utilized in the study to help preserve the slump of the concrete. Table 6 provides a detailed account of the properties of this particular type of superplasticizer.

3.4 Silica fume (SF):

The silica fume (SF) was derived from a powder containing an average of 93% silicon and was manufactured by Sika Egypt. Table 7 displays the chemical and physical characteristics of the SF.

3.5 Aluminum powder (AL):

AVI-CHEM laboratories and Amargain Industrial Complex Company in Egypt produced

Table 8 Physical and Mechanical Properties of Aluminum powder (AL)

Specific gravity	2700 kg/m^3
Melting point	660C
color	silver
form	powder

Table 9 Chemical and physical properties of silica fume (SF)

Specific Gravity	2120 kg/m^3	AL2O3	27.65%
Sio_2	56.88%	CaO	3.6%
Sulphate SO_4	0.27%	MgO	0.34%
Tio_2	0.31%	LO1	4.46%

Aluminum powder (AL), which has an atomic weight of 26.98 ppm and a density of 0.55 g/cm^3. The aluminum powder was evaluated by IS 438-2006 and ASTM B 212-99 (B 212-99 2001). When used as an expansive ingredient, the aluminum powder can cause the physical characteristics of a sand-cement grout to expand before setting. This is due to a chemical reaction that occurs when aluminum powder is added. And, it causes the production of hydrogen gas. As more gas is produced, the grout expands, and the air content increases. Table 8 presents the chemical and physical properties of aluminum powder.

3.6 Fly ash (FA):

Fly ash (FA) had been produced by AR USP Egypt Amargain Industrial Complex Company. Table 9 shows the chemical and physical properties of (FA).

4. Methodology:

The recycled coarse aggregate (RCA) was the primary material used in this study which was produced from a large quantity of pretested concrete cubes provided by construction companies in Egypt. The RCA had a constant ratio of RCA to cement (RCA:C) of 6:1, and the aggregates went through a sieving process before being mixed. The coarse aggregate size used in this study was 20 mm. Various additives were employed in both RC and conventional concrete (AC), including different percentages of (SF) (0%, 10%, 15%, and 20% of the cement amount), as well as (SP) at a 10% cement amount for all mixtures except the reference mixture. Additionally, (FA) and (AL) were gas-forming agent. It is worth noting that concrete containing SF can possess high strength and durability, as evidenced by this experimental study.

5. Mixture design:

This study examined the impact of incorporating silica fume (SF) on the physical and mechanical characteristics of (LWC). The concrete mixtures tested in the experiment were classified into RC and AC. The mixtures were designed to achieve a cubic compressive strength of 14 MPa and an oven-dry density of 1900 kg/m^3 after 28 days, following ASTM (C330-82a) standards. The results

Table 10 Ratios of the ingredients of mixtures LWC (RC)

Mix No.	Cement Kg/m^3	Sand Kg/m^3	RCA Kg/m^3	RCA:C %	w/c%	SF Kg/m^3	SP Kg/m^3
RC r	396	804	846	2:1	0.55	0	0
RC1	141	0	846	6:1	0.55	14	14
RC2	141	0	846	6:1	0.55	22	14
RC3	141	0	846	6:1	0.55	28	14

were compared to those of normal strength concrete made from recycled normal-strength concrete mixes (Fahmy and Idriss 2019) with a water-to-cementitious material ratio of 55%. The study aimed to utilize the potential of SF and FA to enhance the mechanical properties of LWC, including density, compressive strength, tensile strength, percent of voids, and porosity, while investigating the plastic damage behavior of lightweight concrete.

The proportion between aggregates and cement by weight in a concrete mixture is known as the aggregate-to-cement ratio. This fundamental relationship significantly influences the concrete's core characteristics. The interaction between these components serves as a crucial determinant in establishing how strong, manageable, and long-lasting the final concrete product will be. When engineers specify a higher quantity of aggregate in relation to cement, they create what's known as a lean mixture. Such compositions contain reduced cement paste available to coat and bind the aggregate particles, which may result in challenges when working with and placing the concrete. Such mixes, known as lean, enhance the strength by decreasing the concrete's total porosity. Conversely, a lower aggregate cement ratio means a richer mix with more cement paste, leading to better workability and cohesiveness. The aggregate cement ratio influences the strength of concrete; a leaner mix can result in higher strength due to reduced porosity from fewer voids in the paste. However, the strength of concrete is not solely dependent on this ratio (Poon and Lam 2008),(Salain 2021). In addition, the mixtures were designed according to ASTM C330-82a standards (Concreate 2017) to achieve a compressive strength of 14 MPa and an oven-dry density of 1800 kg/m^3 after 28 days. The conventional concrete mix ratio of cement: sand: aggregate was 1:2:4. However, since this study excluded sand, the ratio was adjusted to 1:6 (cement: aggregate) to maintain proportional material distribution.

6. Procedures of mixing preparation:

A drum mixer was utilized to mechanically mix the concrete constituents. Initially, (RCA) and cement were mixed with (SF) for 30 seconds, followed by the addition of half of the mixing water. A pan mixer with a capacity of 0.1 m^3 was then used to prepare all concrete mixtures. Subsequently, (SP) was added to one liter of water at a concentration of 10% by mass of cement to form an aqueous solution. The solution was mixed using a high-speed blender to ensure a uniform distribution of the particles and prevent particle agglomeration due to the strong attractive forces of van der Waals. On the other hand, for the conventional concrete (AC) mixture, a mixture of sand, cement, and SF was used to prepare an aerated concrete mixture. All mixtures were mixed in a rotating drum mixer for two minutes, followed by the addition of 70% of the mixing water along with (AL) and (FA), which were mixed for five minutes. The remaining water was then added and mixed for another 10 minutes.

Table 11 Ratios of the ingredients of mixtures LWC (AC)

Mix No.	Cement Kg/m^3	Sand Kg/m^3	RCA Kg/m^3	RCA:C %	w/c%	SF Kg/m^3	SP Kg/m^3
AC r	400	804	0.55	0	0	0	0
AC1	400	804	0.55	10%C	40	40	0.8
AC2	400	804	0.55	15%C	40	40	0.8
AC3	400	804	0.55	20%C	40	40	0.8

(a) Prepare the materials RC (b) Samples tested cubes RC

Fig. 5 Steps of mixing the LWC with no fine aggregate (RC)

(a) Prepare the materials RC (b) Samples tested cubes RC

Fig. 6 Steps of mixing LWC the aerated concrete (AC)

All mixtures were tested with varying percentages of SF (0%, 10%, 15%, and 20% of cement weight), as shown in Tables 10 and 11. The slump of the fresh concrete mixes was measured using a standard slump test apparatus, while the fresh concrete density and compact factor were studied to investigate the workability of the concrete mix, in accordance with (ECP-203 2007)

The standardization and testing guidelines established by ASTM B212-99 (Funnel 1999) outline specific procedures for determining powder material proportions, particularly concerning SF, FA, and AL ratios, focusing specifically on the apparent density measurement of free-flowing metallic powders. (Paikara and Gyawali 2023) indicated that while aluminum powder effectively reduces

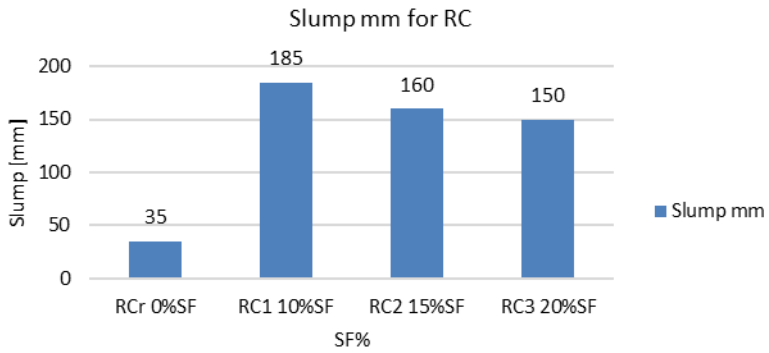

Fig. 7 Slump test [LWC- no fine aggregate RC]

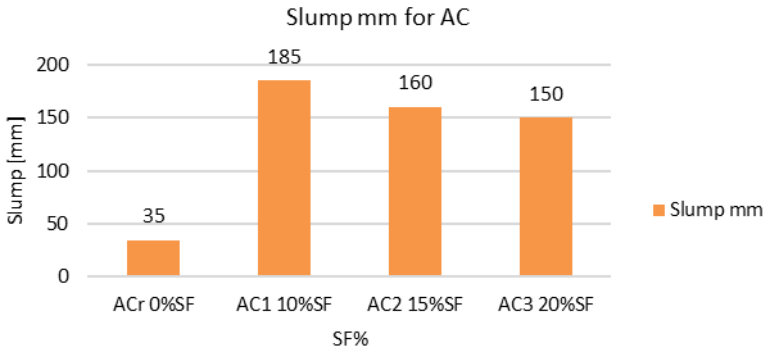

Fig. 8 Slump test [LWC -aerated concrete AC]

concrete density, this comes at the expense of diminished strength parameters and elasticity modulus. Studies (Tanyildizi and Coskun 2008, Chen and Liu 2008) have demonstrated optimal compressive and splitting tensile strength in specimens incorporating 20% silica fume, with these mixtures also exhibiting superior workability characteristics without segregation issues. The selection of FA and SF as supplementary cementitious materials (SCMs) was strategically made to achieve density reduction in concrete applications. In their research, (Almuwbber *et al*. 2018) observed that increased fly ash content correlated with improved concrete flowability, though they noted that excessive FA content adversely affected 28-day compressive strength through dilution effects. In addition, several studies demonstrated that fly ash particles' spherical shape minimizes interfacial friction between aggregates, leading to superior concrete flowability (Zhao *et al*. 2015, Liu *et al*. 2021)

7. Preparation and curing of test specimens

To prepare the test specimens, the first step was to select steel models, and in this experiment, cubic molds measuring 150 x 150 x 150 mm were used. All concrete specimens were cast in layers of approximately 50 mm depth, and a simple rod was employed to compact each layer. However, during mechanical compaction or vibrating processes, the cement paste may flow off the aggregate. The samples tested consisted of 36 cubes measuring 150 x 150 x 150 mm and 9 cylinders measuring

Table 12 Fresh concrete tests

Concrete Type	Test	Fresh concrete test			
	Mix No.	Fresh concrete density (Kg\m^3)	Slump mm	Compact factor	workability
Ordinary concrete	RCr	2000	35	0.95	low
LWC (RC)	RC1	1627	185	1.0	high
	RC2	1509	160	1.0	high
	RC3	1255	150	1.0	high
LWC (AC)	ACr	1800	280	0.95	high
	AC1	1743	275	0.97	high
	AC2	1700	250	0.98	high
	AC3	1650	245	0.98	high

150 mm in diameter and 300 mm in height. After all the materials were prepared, the cubes and prisms were cast according to the design mix. In addition, a slump test was conducted in the fresh state to determine the workability of the concrete mix. The specimens were then placed in their molds at room temperature with a plastic sheet covering to prevent water loss for 24 hours. Afterward, they were carefully removed and immersed in a water tank at a temperature of approximately 23±2°C in the laboratory for 28 days. Fig. 5 illustrates the steps of mixing the concrete for RC, while Fig.6 depicts the mixing process for AC. Before mechanical testing, the specimens were cured in water for 7, 14, and 28 days. Compressive and tensile strength tests were conducted to determine the mechanical behavior of the concrete. Tables 10 and 11 present the ingredient ratios of the mixtures for RC and AC, respectively.

8. Results and discussion:

8.1 Fresh concrete test:

8.1.1 Slump test:

The initial experiment carried out in this study involved a slump test, where the desired range of slump was set between 150 and 200 mm, with the objective of gauging the impact of LWC on workability. The study was divided into two groups, RC and AC, as per the Egyptian Code ECP 203-2007 (2007), and the influence of different levels of SF on workability was examined across all tests. The slumps of RC mixtures with SF percentages of 10%, 15%, and 20% were 429%, 357%, and 329% higher than the reference sample (RCr), respectively. Similarly, the slumps of AC mixtures with SF percentages of 10%, 15%, and 20% were 686%, 614%, and 600% higher than RCr, respectively. The results of the slump test for LWC are presented in Figs 7 and 8. Table 12 provides the values of slump and compaction factors for the various cases of fresh concrete samples.

8.1.2 Compaction test:

The research also included a compaction test, which involved conducting a compacting factor test. This test was carried out to evaluate the extent to which new concrete compacts on its own when allowed to fall without any external compaction. The compaction factor was calculated using Eq. (1).

(a) Compaction test (b) Slump test (c) Air voide test (d) Bulk density test

Fig. 9 the steps of slump and compaction test

$$compaction\ factor = \frac{m1}{m2} \tag{1}$$

where:

M1= Partially Compacted Concrete (Kg)

M2= Fully Compacted Concrete (Kg)

The results indicate that the compaction achieved through free falling is consistent with the standard ECP 203-2007 (2007) Egyptian Code. Furthermore, the findings demonstrate that the compacting factors of all concrete mixtures, including RC and AC, fall within the range of 1.0% to 0.95%. Fig. 9 illustrates the fresh concrete test (a-compaction factor, b-slump test, c-% of air voids and d- bulk density).

8.1.3 Bulk and dry density:

In accordance with the ACI Committee 213, LWC can be classified based on its unit weight or density, which typically ranges from 320 to 1920 kg/m^3 (Aci Committee 2014). On the other hand, normal weight concrete typically has a weight between 2240 and 2450 kg/m^3. The density tests were conducted using the ASTM C138/C138M-14 technique, and the values obtained are presented in Tables 12 and 13. The results indicate that for RC, the density of the concrete decreased within the range of 0.628% to 0.814% from the reference sample RCr. Meanwhile, for AC, the density of the concrete decreased within the range of 0.82% to 0.90% from the reference sample ACr. It is clear from the results that the density decreases with increasing polymer composites with SF. This is due to the function of SF in improving pore structure. SF and FA particles act as fillers, bridging the voids between cement grains and aggregate particles. Moreover, SF reacts pozzolanically with $Ca(OH)^2$ to form a larger solid volume of the C–S–H (calcium silicate hydrate)phase, which further reduces capillary porosity following hydration (Bentz and Stutzman 1994). Fig. 10 illustrates the relationship between the types of concrete mix and the concrete density for RC and AC, expressed as a percentage of density with respect to ordinary concrete (RCr). Additionally, Fig.11 shows the voids ratio and cubic drying test. On the other hand, the bulk density can be calculated using equation 2, according to the ACI Committee 213.

$$Bulk\ density = \frac{[W2 - W0][gm]}{V[cm3]} \tag{2}$$

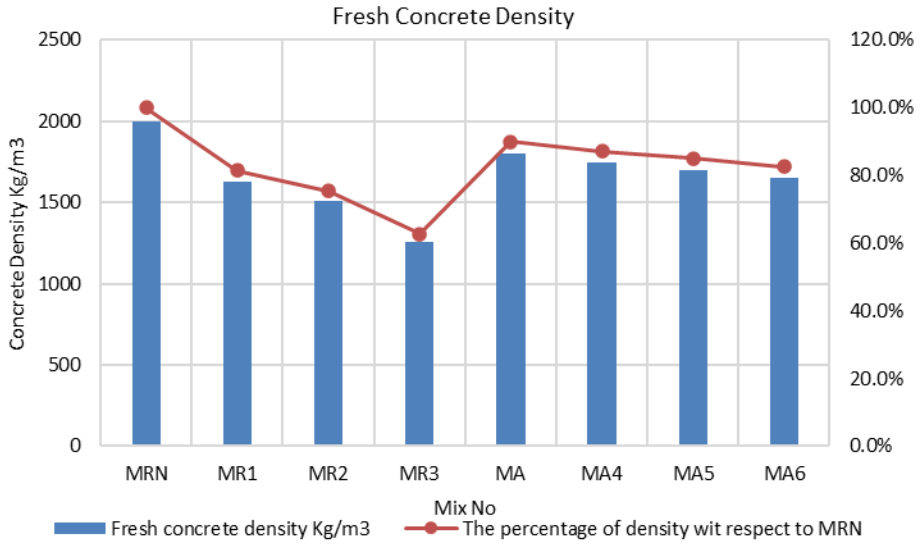

Fig. 10 Fresh Concrete Density

(a) Concrete Porous (b) Oven dried sample

Fig. 11 Voids ratio and cubic drying test

where:

W_2-W0: net concrete weight

W_2: weight compact concrete

Wo weight of density measurement

V: volume

8.1.4 Porosity and void ratio:

Porosity refers to the percentage of the bulk volume of a substance that is occupied by voids (Lee *et al*. 2018). The evolution of the porous network in concrete has a significant impact on its durability. Moreover, the porosity of concrete can affect its mechanical strength and other properties. When the porosity of concrete is high, particularly if the pores are large in diameter and interconnected, it can negatively impact its strength and permeability (Van *et al*. 2019).

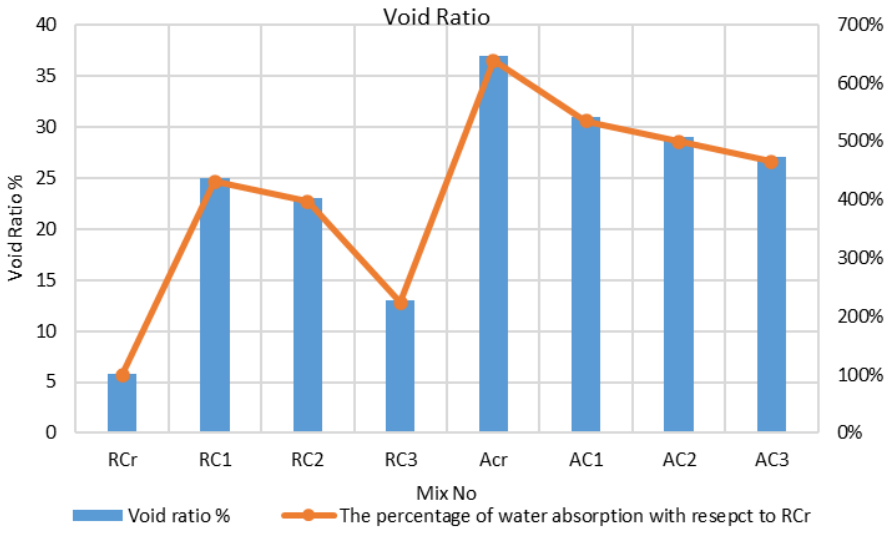

Fig. 12 Void Ratios of Concrete Mixes

Table 11 Ratios of the ingredients of mixtures LWC (AC)

Mix No.	Cement Kg/m^3	Sand Kg/m^3	w/c%	SF	SP Kg	FA Kg	AL Kg
AC r	400	804	0.55	0	0	0	0
AC1	400	804	0.55	10%C	40	10%C	0.2%C
AC2	400	804	0.55	15%C	40	10%C	0.2%C
AC3	400	804	0.55	20%C	40	10%C	0.2%C

Most researches use Eq. (3) to calculate the porosity of no-fines concrete (Park and Tia 2004).

$$\text{Void Ratio } \eta = 1 - \left[\frac{Weight\ Under\ Water - over\ Dried\ Weight}{Density\ of\ Water}\right] x\ [Volume\ of\ Sample] \quad (3)$$

Porosity (e): it is defined as the ratio of the volume of voids to the total volume of mortar as shown in Eq. (4).

Hence,

$$e = \eta(1 + \eta) \quad (4)$$

On the other words, porosity refers to the ratio of the volume of voids to the total volume of a substance, while the void ratio η is the proportion of void volume to the total solids volume. Fig. 12 and Table 13 illustrate the void ratios for different concrete mixes and highlight the differences between the results for (RC) and (AC). The experiment was conducted with a fixed mix proportion, aggregate/cement ratio of 6:1, and water/cement ratio of 0.55, but with varying content of silica fume as a pozzolanic effect to reduce voids. As shown in Fig. 12, ACr and AC1 have void ratios that are 538% and 434% larger than the reference sample [RCr], respectively. On the other hand, RC1 and RC2 have void ratios that are 331% and 297% larger, respectively. The results demonstrate that RC and AC have significantly different values from normal concrete RCr. As porosity increases, permeability also increases, and water tends to flow and occupy space in concrete microstructures,

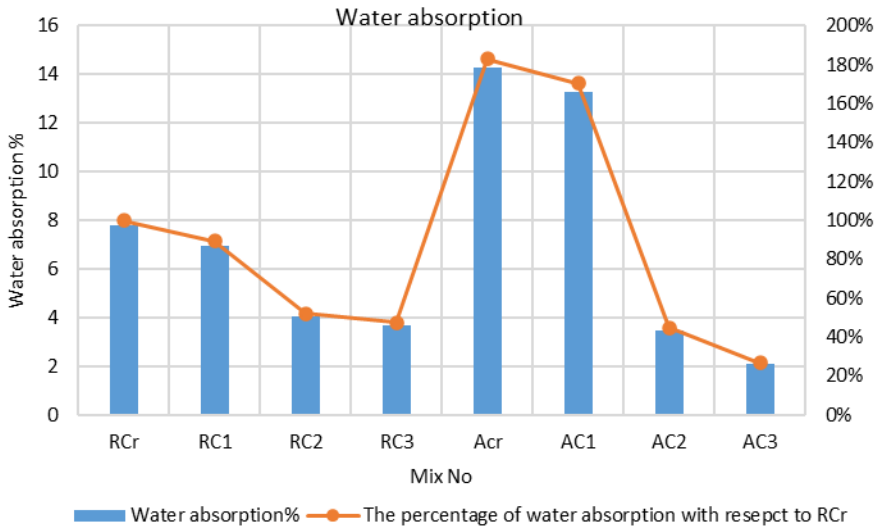

Fig. 13 Water absorption

which can affect the relative density when the water evaporates (Lian *et al*. 2011). Furthermore, increasing the amount of silica fume leads to a decrease in void ratio. In contrast, AC1, AC2, and AC3 have a decrease in their void ratios by 16.22%, 21.62%, and 27.03%, respectively, with respect to ACr (SF=0). In contrast, the AC group has a larger void ratio than the RC group. This is because the AC group had a constant ratio of AL with FA content, and the void ratio and porosity of the LWC decreased systematically with increasing polymer composites containing SF due to the formation of a high amount of pores. The percentage of decrease in void ratio due to increasing SF ranges from 16% to 31%.

8.1.5 Water absorption:

To assess the water absorption capacity of lightweight aggregate concrete in both RC and AC, this research utilized a water absorption test as the first step. The test required taking the specimen cubes out of the curing tank two weeks earlier than planned and drying their surfaces before weighing them to determine their dry weight. All water absorption tests adhered to the standard [BS1881-122], and Eq 5 can be applied to compute the water absorption values.

$$W.A = \frac{\text{Wwet} - \text{Wdry}}{Wdry} * 100\ \% \tag{5}$$

where:

W.A: water absorption

Wwet = wet weight of specimen,

W_{dry} = dried weight of specimen

The absorption capacity, or moisture content, was determined by weighing a surface-dry sample after it had been evened for 4 hours, and then weighing it again after it had been dried in an oven. The difference in weight between the two measurements represents the absorption capacity. All water absorption tests were conducted in accordance with the [BS1881-122] standard. Fig. 13 shows the relationship between the water absorption of mortar cubes with different polymer composites

Table 13 Hardened concrete tests

LWC Type	Test Mix No.	Compressive strength (MPa)			Tensile strength (MPa)	Void ratio %	Water absorption%	Bulk density (kg/m^3)
		7 day	14 day	28day	14 day	28 day	28day	28day
RC (no sand)	RCr	4.62	7.10	14.1	1.10	5.8	7.80	2800
	RC1	0.45	0.82	1.80	0.80	25	6.97	430
	RC2	1.20	1.70	3.50	1.10	23	4.06	615
	RC3	2.60	4.50	5.60	1.20	13	3.70	810
AC	ACr	5.80	6.50	8.30	1.0	37	14.28	1410
	AC1	7.10	9.10	9.90	1.20	31	13.3	1500
	AC2	6.10	10.10	12.90	1.25	29	3.50	1450
	AC3	6.40	10.05	14.30	1.30	27	2.08	1440

and SF proportions over curing days. The results indicate that the water absorption of the cubes gradually increases until the 28th curing day. However, RCr has a higher percentage of water absorption than RC1, RC2, and RC3, while ACr has a higher percentage of water absorption than AC1, AC2, and AC3. The results highlight a significant decrease in water absorption due to the increased dosage of silica fume, suggesting that a high concentration of silica fume can act as a mortar filler and minimize the holes between particles. In other words, a high content of polymer composites with SF silica fume can reduce the pores between particles, and the (SF) can act as the mortar's filler. Additionally, the water absorption decreases as the percentage replacement of silica fume increases. Fig. 13 illustrates the water absorption ratio for RC and AC and shows the differences in findings between them. ACr and AC1 have values that are 83% and 71% larger than the reference sample RCr and RC1, respectively. On the other hand, AC2, AC3, RC2, and RC3 have values that are smaller than RCr by 73%, 55%, 53%, and 48%, respectively.

8.1.6 Compressive strength:

The concrete cube test is widely used to determine compressive strength for quality control. Fig. 14 shows the compressive strength of RC and AC after 7, 14, and 28 days. According to the findings presented in Fig. 14, the compressive strength of reinforced concrete (RC) increases as the proportion of silica fume in the cement content increases, with percentages ranging from 10% to 20%. The increase in compressive strength is observed to range from 1.8 MPa to 5.6 MPa. In other words, the compressive strengths of zero percentage aluminum powder, 10% Sikament, and RC mixtures increase with increasing SF. Additionally, there is a decrease in compressive strength by 87%, 75%, and 60% from the value of RCr. On the other hand, it can be observed that as the amount of SF in the concrete increases, the compressive strength of the concrete also increases for AC. The compressive strength of 10% Sikament, 10% FA, 0.2% AL with 20% SF is more than 72% higher than the value of the same specimen without SF, increasing from 9.9 to 14.3 MPa. The value for AC3 has nearly the same compressive strength value as RCr. Therefore, the compressive strength in LWC can be increased by increasing SF to reach the same value as ordinary concrete. Furthermore, it can be seen that the decrease in compressive strength for AC1 and AC2 is 29.8% and 8.5%, respectively, from the value of RCr. This gives better results than RC. Fig.15 demonstrates the rate of compressive strength gain from 7 days to 28 days. The results confirm that the rate of

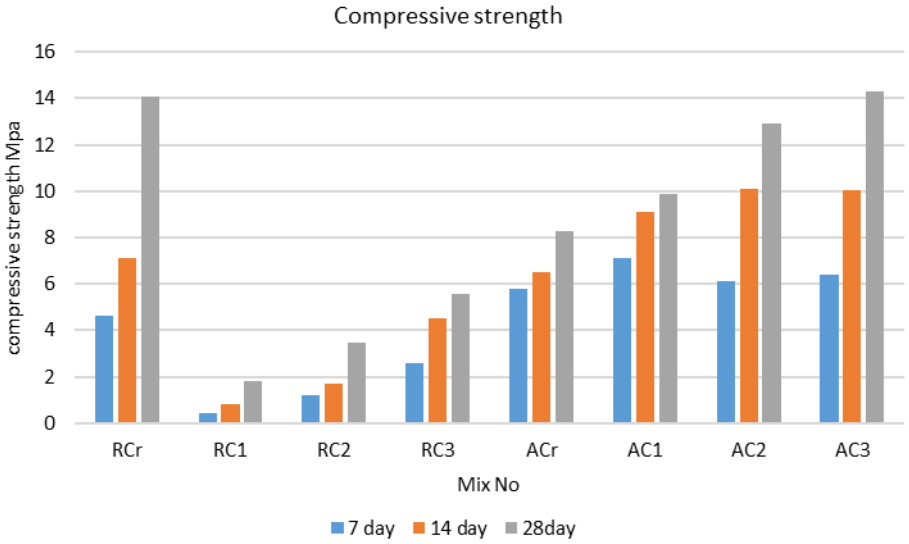

Fig. 14 LWC compressive strength Mpa

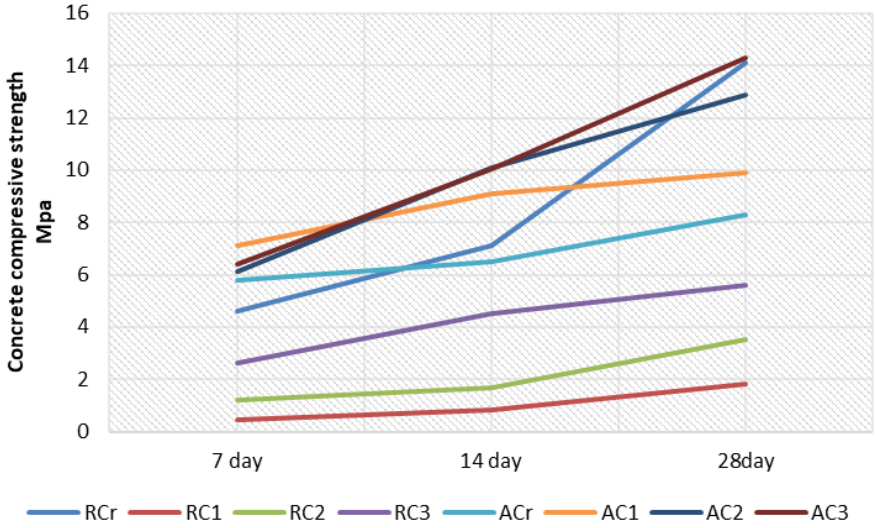

Fig. 15 Concrete compressive strength for LWC after [7day,14day and 28day]

compressive strength increase up to 7 days is higher than from 7 to 28 days because SF reacts quickly and provides early strength. The pozzolanic action of silica fume provides an increase in compressive strength at 7 days that is larger than that seen at 28 days (Narattha *et al*. 2015)

The results depicted in Fig.15 indicate a marginal rise in the compressive strength of the concrete over a period of 7 to 28 days. This trend is observed as the content of silica fume in the concrete increases from 10% to 20%, resulting in an increase in compressive strength from 9.9 MPa to 14.3 MPa. The compressive strength of the samples is directly related to the SF content, as demonstrated in Figs 16 and 17. However, this trend is typically only observed when the percentage is increased from 0% to 20%. Figs 18 and 19 illustrate the compressive tests for the first and second groups.

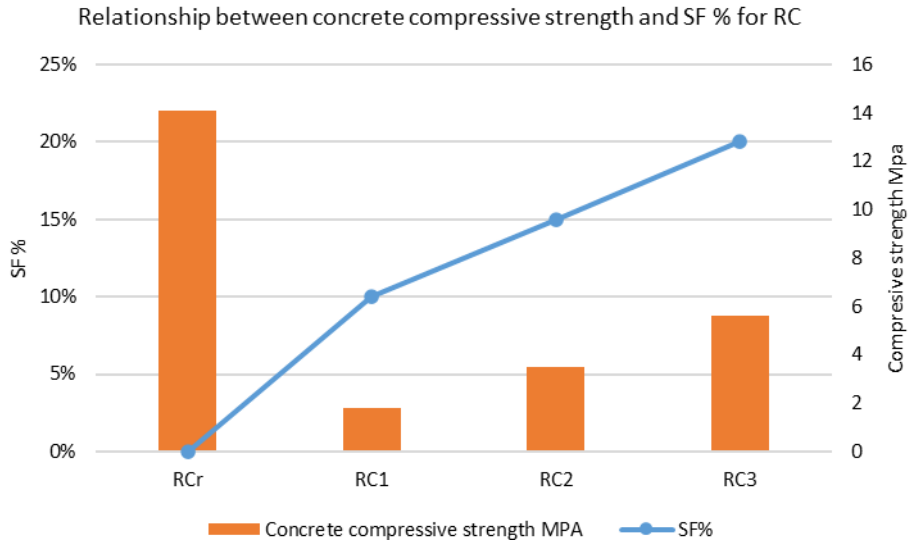

Fig. 16 Relationship between concrete compressive strength and SF % [no fine concrete RC]

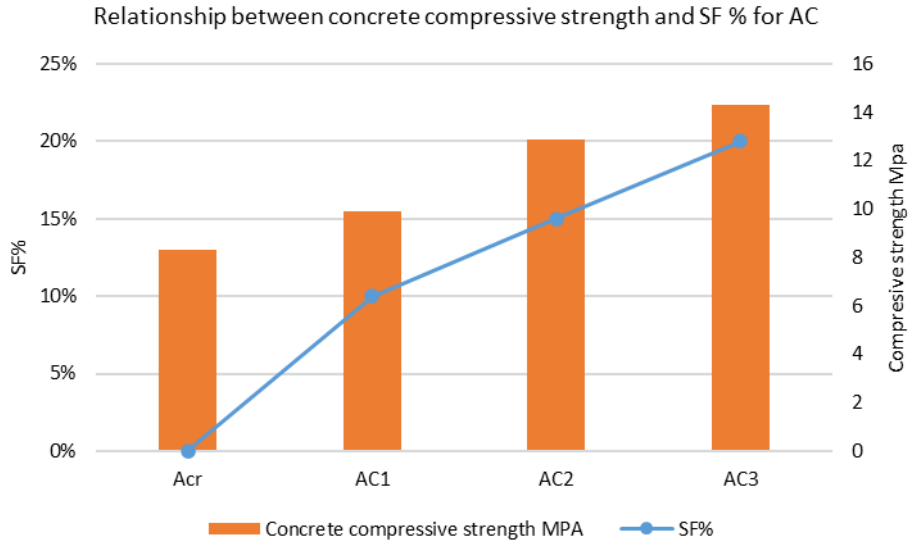

Fig. 17 Relationship between concrete compressive strength and SF % LWC (AC)

Based on the findings, the optimum proportion that produced the highest compressive strength is 20% of silica fume in aerated concrete. In other words, the value for 20% SF is nearly the same as ordinary concrete RCr as a reference sample. However, for SF at 10% and 15%, the compressive strength decreased by 87% to 60% for RC and 29% to 8.5% for AC.

8.1.7 Splitting tensile strength:

The splitting tensile strength of both RC and AC after 14 days is illustrated in Fig. 20. The experimental results indicate that the percentage of silica fume (SF) content has a significant effect

(a) Curing cube (b) Compressive test (c) Concrete section

Fig. 18 Compressive Test for First Group [RC]

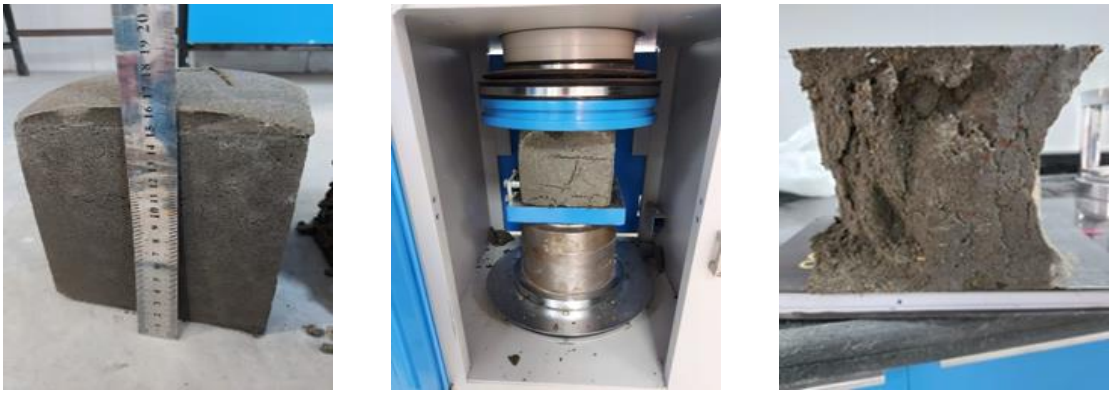

(a) Curing cube (b) Compressive test (c) Concrete section

Fig. 19 Compressive Test for Second Group [AC]

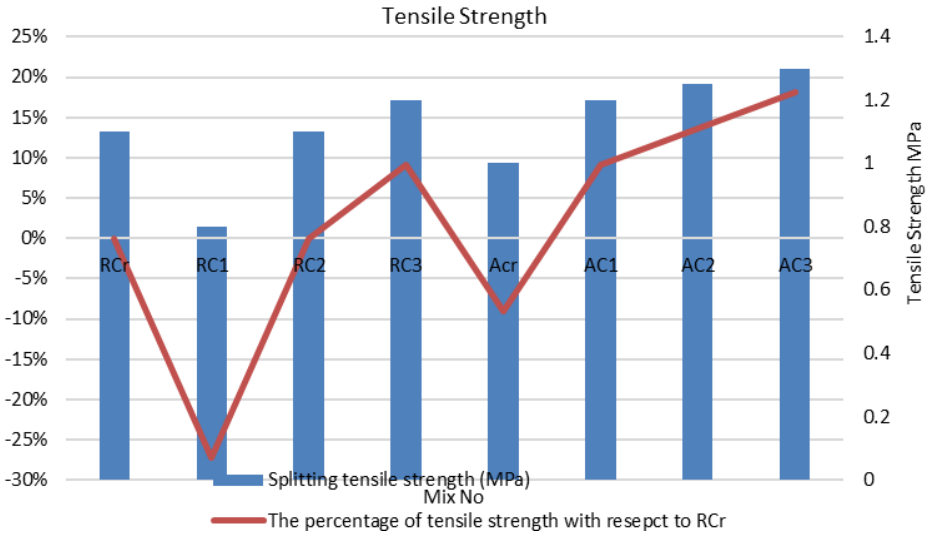

Fig. 20 Splitting tensile strength

(a) Cylinder sample (b) Tensile test (c) Concrete section

Fig. 21 Splitting tensile test for [RC]

(a) Cylinder sample (b) Tensile test (c) Concrete section

Fig. 22 Splitting tensile test for [AC]

on the splitting tensile strength of RC specimens. An increase in the proportion of SF in the cement content, ranging from 10% to 20%, is observed to enhance the tensile splitting strength of RC specimens, with a rise in strength from 0.8 MPa to 2.2 MPa, as depicted in Fig. 20. The values of tensile strength for RC3 are bigger than RCr by 9%. However, RC1 shows a decrease in strength by 27% compared to the reference sample RCr. Therefore, increasing the percentage of SF up to 20% has a significant effect on increasing tensile strength. In contrast, with regards to non-reinforced concrete (AC), an increase in silica fume (SF) content is also observed to result in an increase in tensile strength. Specifically, the tensile strength of AC specimens containing 10% Sikament, 10% fly ash, and 0.2% SF, with 20% silica fume, is more than 18% higher than the value of the reference sample RCr. This suggests that the addition of SF can significantly enhance the tensile strength of AC.

The incorporation of pozzolanic materials demonstrated a positive correlation with enhanced tensile strength in lightweight concrete (LWC) specimens. In aluminum-containing lightweight concrete (AC-LWC), the aluminum content generated significant void formation, while the reinforced lightweight concrete (RC-LWC) was characterized by the absence of sand. The increased

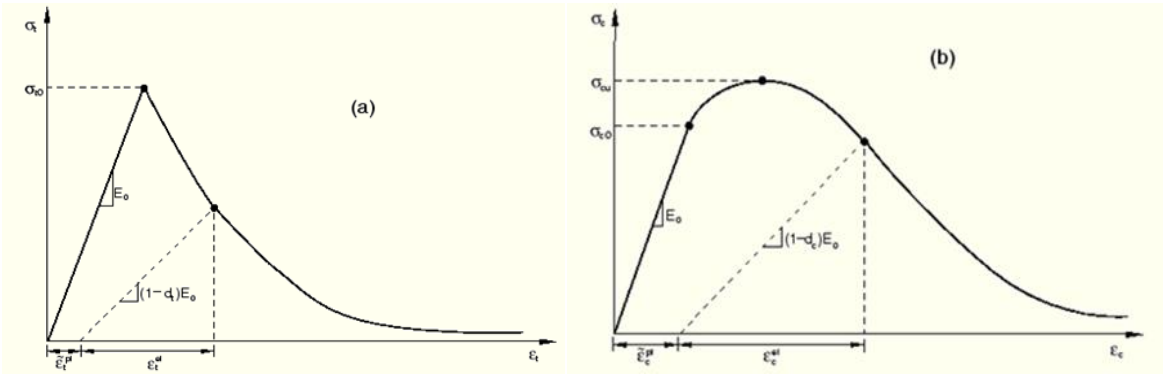

Fig. 23 Response of concrete to uniaxial loading in tension (a) and compression (b) ABAQUS (Manual 2012)

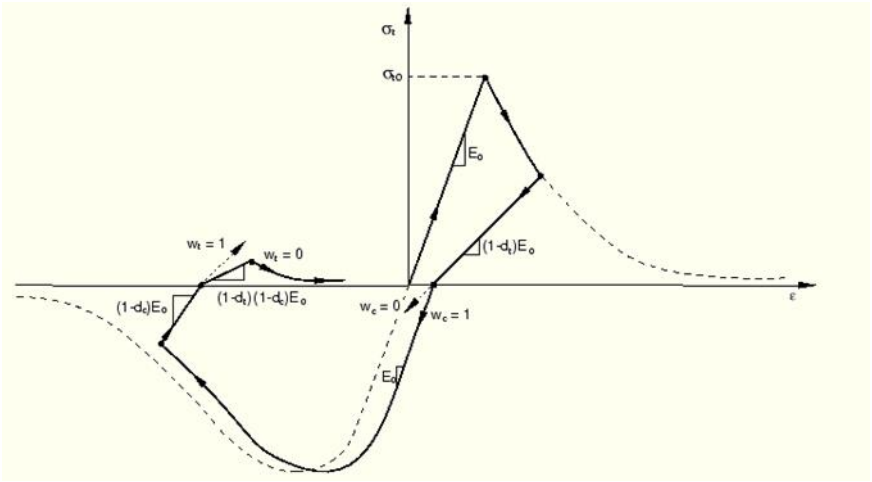

Fig. 24 Uniaxial load cycle (tension-compression-tension) ABAQUS (Manual 2012)

silica fume (SF) content served as void-filling particles, influencing the cellular structure of the lightweight concrete matrix. The enhancement in mechanical properties can be attributed to the densification of the microstructure, where nano and micro particles effectively filled the interconnected pores. This process facilitated improved hydration product formation, leading to expansion of the calcium-silicate-hydrate (CSH) gel and a reduction in pore dimensions, ultimately contributing to superior tensile strength development (Różycka and Pichór 2016, Kunchariyakun *et al*. 2015, Shabbar *et al*. 2024).

As a result, there was an increase in splitting tensile strength from 1.0 to 1.3 MPa. However, the values of tensile strength for AC are greater than those for RC. Figs. 21 and 22 illustrate the splitting tensile strength for RC and AC. Furthermore, the initial yield stress in compression is a factor of 10 or more higher than the initial yield stress in tension.

8.2 ABAQUS/Standard damaged plasticity model for concrete

When the concrete specimen is unloaded from any point on the strain softening branch of the

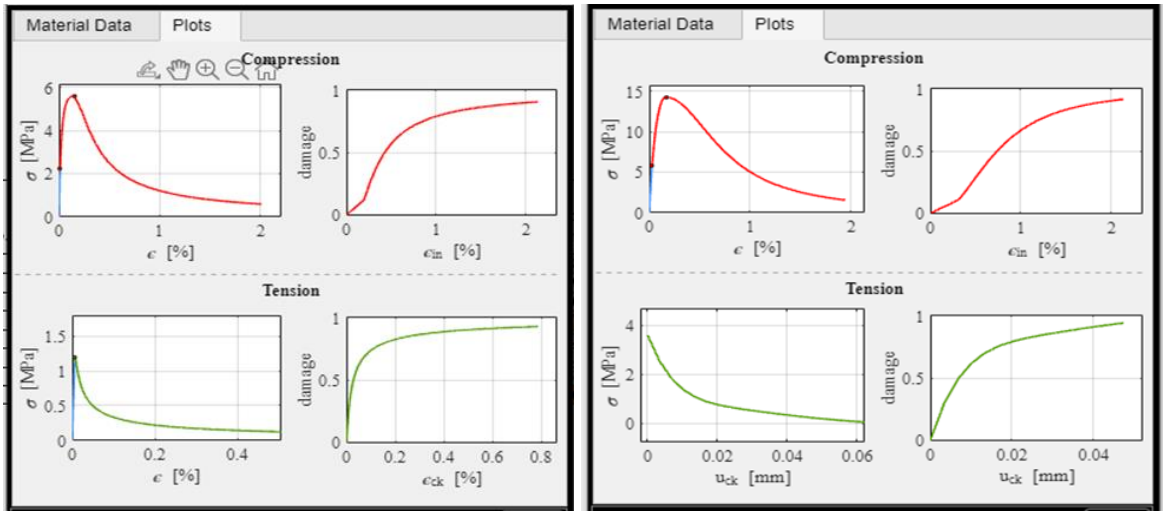

RC3 AC3

Fig. 25 CDP Input Generator

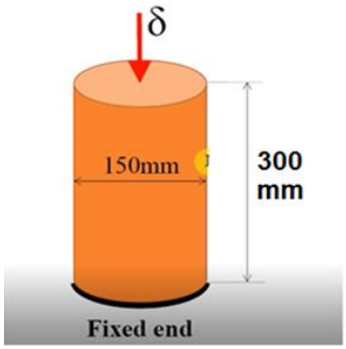

Fig. 26 The configuration of the tested concrete compression cylinder

stress-strain curves, the unloading response is observed to be weakened and the elastic stiffness of the material appears to be damaged (or degraded) as shown in Fig. 23. The degradation of elastic stiffness shows a notable distinction between tension and compression tests, but in both cases, the impact is more evident with an increase in plastic strain. On the other hand, the tensile stiffness is not recovered as the load changes from compression to tension once crushing micro-cracks have developed. This behavior, which corresponds to w_t=0.0 and w_c=1.0, is the default used by ABAQUS. Fig. 24 depicts a uniaxial load cycle that assumes the default behavior, while Fig.25 displays the ABAQUS CDP model for RC3 and AC3.

8.2.1 Numerical modeling

The concrete compression cylinder used in the numerical model has a diameter of 150 mm and a length of 300 mm, with a fixed base and displacement control at the top. Material properties for each numerical case with 0.2% by cement weight (SF) are provided in Fig. 26 and Table 13 for case

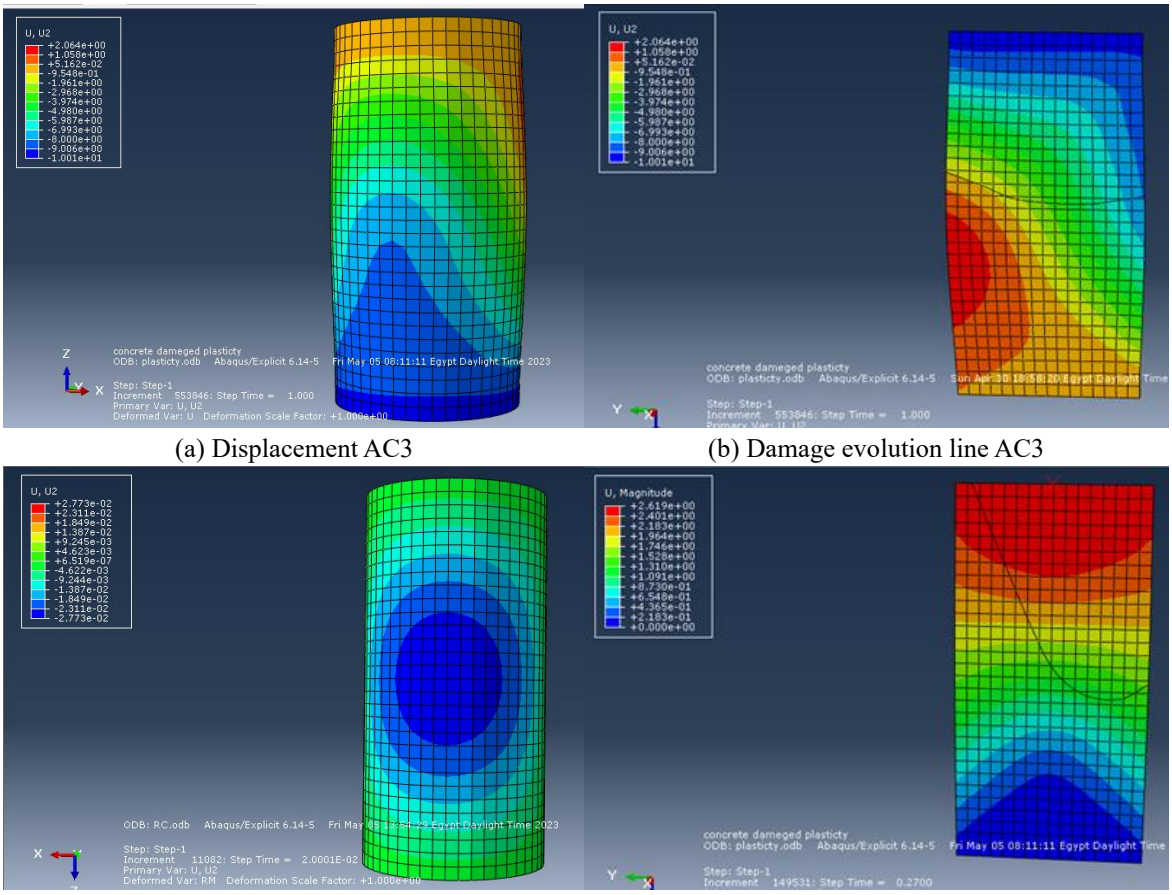

(a) Displacement AC3 (b) Damage evolution line AC3

(c) Displacement RC3 (d) Damage evolution line RC3

Fig. 27 Damage evolution of LWC compression cylinder

1 without fine aggregate (RC3) and case 2 with aerated concrete (AC3). The load was applied by prescribing a maximum vertical displacement at the reference point of a rigid body located on top of the concrete compression cylinder, where the axial loading was actually applied using ABAQUS/Explicit.

8.2.2 Finite element modeling

In the analysis, material properties of lightweight concrete (LWC) with recycled aggregate (RC) and aerated concrete (AC) were obtained from a previous experiment (Şeker *et al*. 2022, Kim *et al*. 2012, Wee *et al*. 2006, Standard 2014), and damage variables were employed to represent tensile and compressive damage independently in the concrete damage plasticity (CDP) parameters. The parameters were calculated based on the stress-strain compression loading relationship. Plastic damage was implemented on the compression cylinder specimens for both LWC samples, with the first sample being RC3 without sand and the second sample being AC3 with dense meshes. In the comparison with corresponding simulations, numerical analysis was used for two different meshes, namely RC3 and AC3. The deflections of the meshes are also displayed for various displacements in both RC3 and AC3. Fig. 27 illustrates the difference between the two meshes, with damage

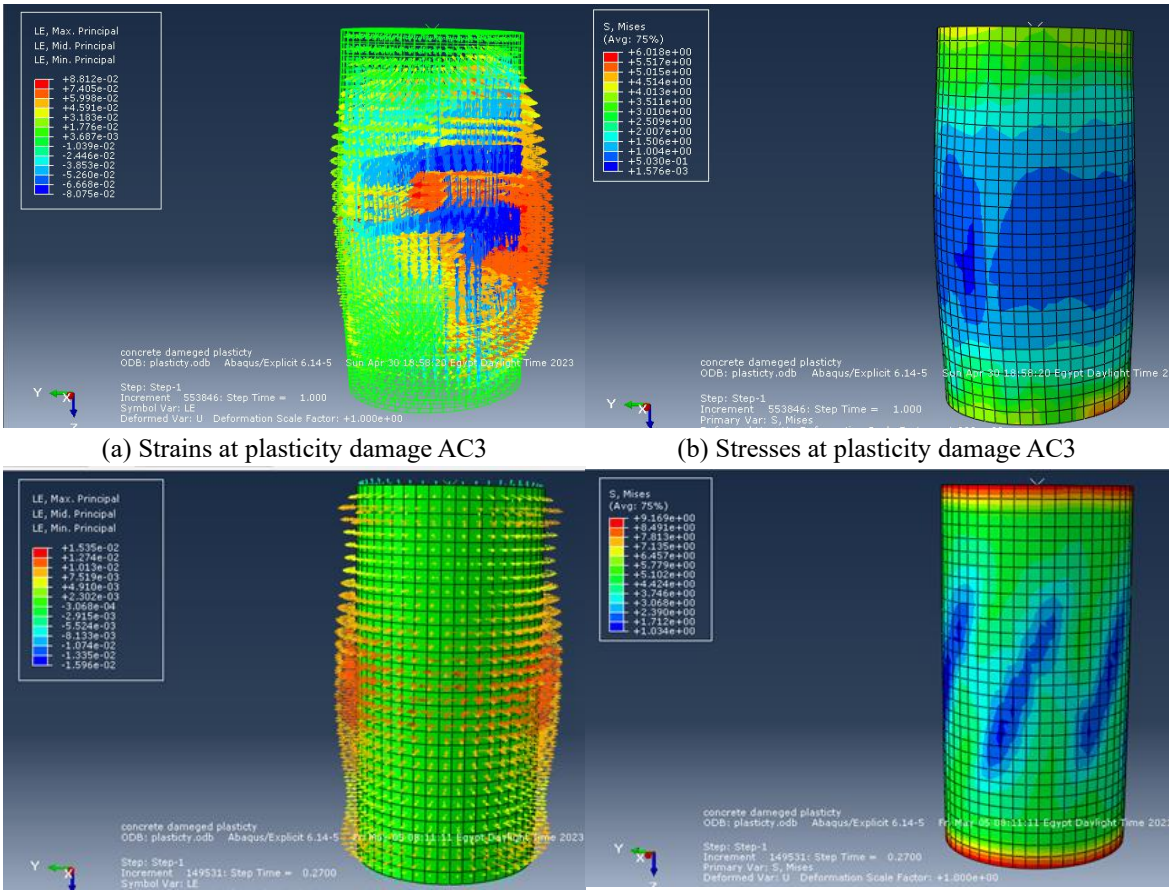

(a) Strains at plasticity damage AC3 (b) Stresses at plasticity damage AC3

(c) Strains at plasticity damage RC3 (d) Stresses at plasticity damage RC3

Fig. 28 Damage versus strain, and stresses versus damage for both cases RC3 and AC3

initiation occurring at 0.0273 mm and 0.0954 mm displacement for RC3 and AC3, respectively. These values are attributed to the LWC samples.

The load versus displacement, stress versus strain, damage versus strain, and strain versus damage results are presented in Fig. 28, along with the damage evolution in all cases considered. The results of the finite element analysis (FEA), which were conducted using the developed constitutive and damage plasticity models, are in good agreement with the experimental outcomes, with less than 10% discrepancies for lateral resistance and accurate predictions of tensile strength. Therefore, the proposed constitutive model and the derived concrete damage plasticity parameters are suitable for use in numerical simulations and finite element modeling of structural concrete.

8.3 Stress strain curve for LWC as RC3 and AC3

Fig. 29 displays the correlation between applied stress and strain for both cylinders. The elastic behavior of both cylinders was approximately similar, with the yield of the RC3 cylinder being 5% lower than that of the AC3. Following yield, the RC3 cylinder exhibited damage cracks, and

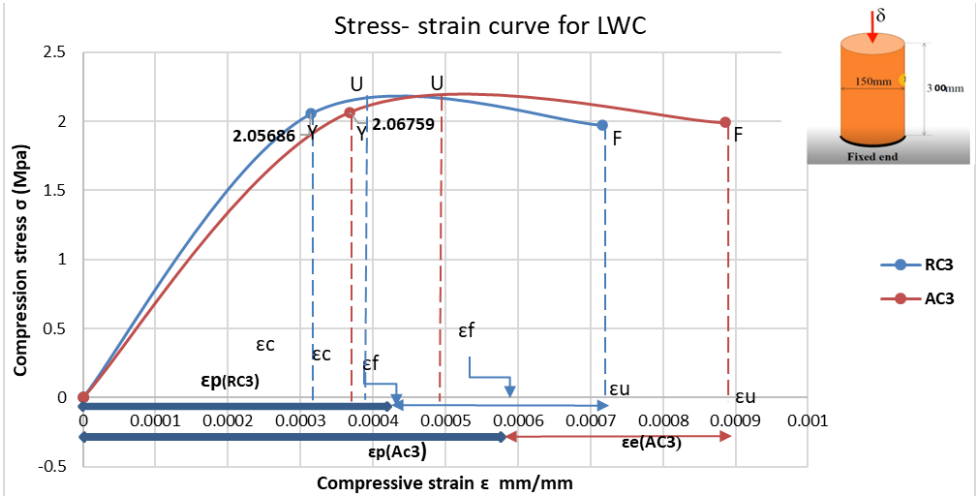

Fig. 29 Stress-Strain curve for LWC (AC3 and RC3)

excessive deformability was observed, resulting in a maximum deflection of approximately 0.00025 mm. On the other hand, the AC3 cylinder demonstrated greater resistance to deformability and a lower rate of increase in deformability with the increase in axial stresses. This further confirms the impact of SF on the LWC of AC. The strength of the RC3 cylinder was 5% lower than the expected shear strength, which may be attributed to the extensive shear cracking observed in this sample.

8.3.1 Elastic and plastic strain

Fig. 29 demonstrates that after a material undergoes yielding, it enters a phase of significant plastic deformation. As the material yields, it also undergoes strain hardening, which raises the strength of the LWC material. The stress-strain diagrams below illustrate an increase in the material's strength between the yield point Y and the ultimate strength at point U, which is due to strain hardening.

Following the ultimate strength at point U, the reduction in cross-sectional area leads to a decline in load-carrying capacity that exceeds the strength increase resulting from strain hardening. As a result, between the ultimate strength at point U and the fracture point F, the engineering strength of the LWC material decreases, and necking occurs. In Fig. above, both elastic and plastic strains are present in the material. If the load is removed at the designated point (σ, ε), the material's stress and strain will follow the unloading line shown.

The elastic strain (ε_e) and plastic strain(ε_p) are indicated in the Fig. 28

$$\text{Elastic strain} \qquad \varepsilon e = \delta \div E \tag{7}$$

$$\text{Plastic strain} \qquad \epsilon p = \varepsilon - \varepsilon e \tag{8}$$

The stress at the indicated point is denoted by σ, the strain at the indicated point is denoted by ε, and the elastic modulus is denoted by E. It is evident that the plastic strain at the point of failure, ε_f, is the residual strain that remains in the material after the recovery of elastic strain. The total strain at failure, which is the sum of the plastic strain and the elastic strain, is known as the ultimate strain, ε_u.

8.3.2 Ductility and toughness

Ductility refers to a material's ability to endure plastic strain before fracturing. A ductile material can sustain significant strains even after yielding has commenced. The ductile LWC material can still bear a load even after reaching the ultimate strength as shown Fig. 29. Common methods of measuring ductility include percent elongation and reduction in area. On the other hand, the area under the stress-strain curve is referred to as toughness. According to an analysis of samples using ABAQUS, AC3 is 17% tougher than RC3.

8.4 Statistical analysis:

The correlation curve for all variable values [compression, tension, and strains] can be obtained using regression analysis, which involves a set of statistical procedures used to establish the relationship between these variables. Before reaching any conclusions, it is crucial to evaluate the assumptions and constraints of the regression model. Nonlinear regression, unlike linear regression, involves fitting a curve or function to the data instead of a straight line. The form of non-linear regression models can vary significantly, depending on the specific relationship between the variables under investigation. Non-linear regression can be accomplished through various techniques, such as polynomial regression, exponential regression, logistic regression, and several others. The selection of an appropriate method is contingent on the particular nature of the relationship being examined and the research question at hand. Before selecting a regression method, it is crucial to evaluate the linearity of the relationship between the variables. This can be achieved by analyzing scatter plots or utilizing statistical tests like the correlation coefficient. If the relationship is evidently non-linear, non-linear regression should be utilized instead of linear regression. In our study, we employed two regression analysis techniques, namely polynomial regression and exponential regression. R-squared (R^2) is a statistical metric that quantifies the proportion of variance in the dependent variable accounted for by the independent variable(s) in a regression model. It serves as an indicator of the goodness of fit of the regression line to the data. R^2 values range from 0 to 1, with 0 indicating that the model explains none of the variance in the dependent variable, and 1 indicating that the model explains all of the variance in the dependent variable. Typically, a higher R^2 value signifies a superior fit of the model to the data. Fig. 30 reveals that the correlation curve closely aligns with the variable data, with R-squared values ranging from 0.8 to 1.0, indicating a strong correlation. Hence, it can be concluded that all equations that articulate the relationship between the values can be utilized to determine the values of tension and concrete compressive strength in lightweight concrete. Eq. 9 expresses the relationship between concrete compressive strength and tensile strength for recycled coarse concrete, while Eq. 10 represents the same relationship for aerated concrete. The study employs statistical regression analysis to derive the equation that signifies the relationship between F_c and F_t for both AC and RC, as shown in Fig 30. which encompass high strength values from all samples. Firstly, the equation that expresses the relationship between concrete compressive strength and tensile strength after 14 days of testing the samples is obtained for both AC and RC cases.

$$\text{For} \qquad \text{RC: } f_t = 0.2278 \ln(fc) + 0.8939 \tag{9}$$

$$\text{For} \qquad \text{AC: } ft = 0.7176 \ln(fc) - 0.3834 \tag{10}$$

Next, the equations between compressive strain and compressive stress are obtained from the curve that is derived from the analysis at Eq.11,12 measurements of ABAQUS for the cylindrical elements as shown in Fig. 30.

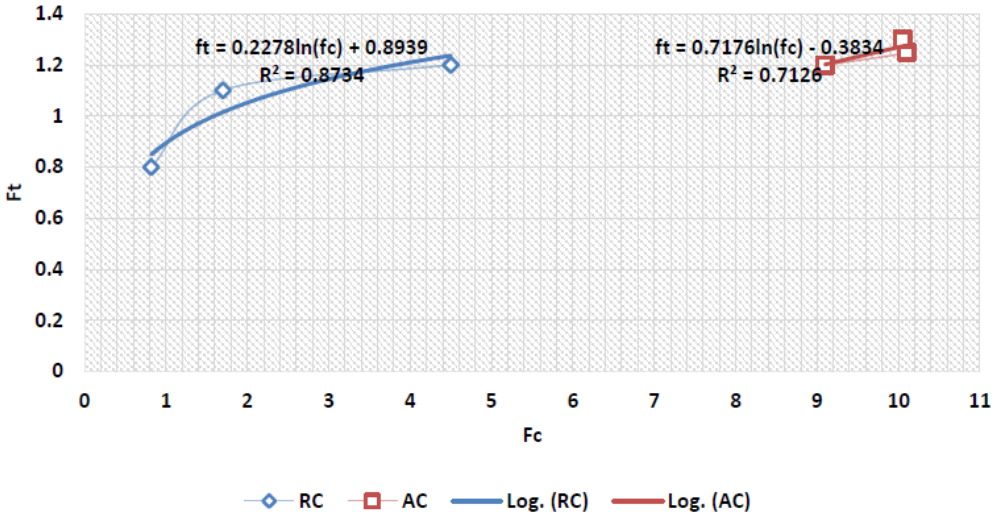

Fig. 30 relationship between Fc and Ft for [RC, AC] Samples

$$\text{For} \qquad \text{RC3: } \sigma = -9 * 10^{6} * \varepsilon^{2} + 9505\,\varepsilon \tag{11}$$

$$\text{For} \qquad \text{AC3: } \sigma = -7 * 10^{6} * \varepsilon^{2} + 8017.6\,\varepsilon + 3 * 10^{-12} \tag{12}$$

where, σ is the compressive stress and ε is compressive strain

Through the compressive testing of cubic samples, the compressive stress-strain relationship of two types of LWC, namely LWC-RC and LWC-AC, which contain distinct combinations of SF and FA, was investigated experimentally. Additionally, regression formulas for compressive and tensile strength were developed, and an elastic-plastic strain cylinder model was established for both LWC-RC and LWC-AC. As a result, the failure modes were influenced by the type of LWC, with notable modifications observed upon the addition of SF. Hence, the following conclusions can be drawn:

9. Conclusions

For experimental concrete test enhanced the effect of SF on LWC

• For RC and AC containing different percentages of SF (10%, 15%, and 20%), the slump values were found to be considerably higher than those of the reference sample of ordinary concrete, RCr, by 429%, 357%, and 329% for RC1, RC2, and RC3, respectively. The slump values for AC1, AC2, and AC3 were also higher, but to a lesser extent, at 1.78%, 10.71%, and 12.50%, respectively. Moreover, it was observed that the slump values decreased as the amount of SF increased in RC, while in AC, the slump values increased with an increase in FA and SF.

• The compacting factors for all concrete mixes of RC and AC were found to range from 1.0% to 0.95%, indicating that SF and FA had no significant impact on the compacting behavior.

• The results indicate that the density of AC decreases as the SF and FA content increases, while for RC, the density increases with an increase in SF. This is attributed to the role of SF and FA in enhancing the pore structure. Due to their small particle size, SF and FA particles fill the gaps

between cement grains and aggregate particles, acting as a filler and bridging the voids.

• The increase in porosity resulting from the addition of SF and FA leads to an increase in permeability, allowing water to flow and occupy spaces within the concrete microstructure. This could potentially affect the relative density upon evaporation of the water. Additionally, the increase in SF content led to a decrease in the air void ratio for both AC and RC, while FA had no apparent effect on the air voids. On the other hand, AC1, AC2, and AC3 showed a reduction in void ratio of 16.22%, 21.62%, and 27.03%, respectively, in comparison to ACr.

• The water absorption significantly decreases with an increase in the SF dosage for both AC and RC. This suggests that high concentrations of SF can act as a filler, filling the gaps between particles, thereby minimizing the formation of voids. However, in the case of AC3, the use of FA resulted in a 43.7% decrease in water absorption compared to RC3.

• The addition of SF with FA resulted in an increase in compressive strength for both RC and AC, with a greater improvement observed in AC compared to RC. Specifically, the compressive strength increased from 1.8 MPa to 5.6 MPa for RC and from 9.9 MPa to 14.3 MPa for AC. Notably, the compressive strength of AC3 was more than 72% higher than that of ACr, while the compressive strength of RC3 was more than 150% higher than that of RCr, which refers to the same specimen without silica fume.

• In the case of RC, the splitting tensile strength of all specimens was affected by the percentage of SF and FA content. The splitting tensile strength of RC3 was found to be higher than that of the other specimens, which is particularly crucial in structural loads where concrete is vulnerable to tensile cracking. Moreover, the splitting tensile strength of RC increased with an increase in SF content relative to the cement content.

• An increase in the SF percentage, up to a maximum of 20%, was found to have a significant impact on the increase in tensile strength. Similarly, for AC, an increase in SF content led to an increase in tensile strength, with AC3 exhibiting a tensile strength value more than 27% higher than that of ACr. Tensile strength is a crucial factor in resisting rupture and tension loads, and the ability to withstand such loads is essential. The tensile strength of RC3 was found to be 41% higher than that of AC3. Finally, FA was observed to decrease the tensile strength in LWC.

In contrast, the results demonstrate a more significant improvement in AC than in RC.

For numerical study the effect of SF on PCD for LWC types:

• The reduction in elastic stiffness was found to vary significantly between tension and compression tests, as predicted by ABAQUS. In both cases, the effect was more pronounced with an increase in plastic strain.

• The numerical analysis was employed to compare the corresponding simulations of RC3 and AC3 at displacement values of 0.0273 mm and 0.0954 mm, respectively.

• In the stress-strain curve for LWC, such as RC3 and AC3, the yield of the RC3 cylinder was found to be 5% lower than that of the AC3 cylinder. This difference in yield strength can be attributed to the observed intensive shear cracking of the RC3 samples.

• In both RC and AC, there is an increase in elastic and plastic strain between the yield point (Y) and the ultimate strength point (U). This increase in strength is attributed to strain hardening.

• LWC exhibits high ductility and toughness, allowing it to withstand significant strains even after yielding. Notably, AC3 showed a toughness value 17% higher than that of RC3.

• A statistical regression analysis was conducted to derive an equation that represents the relationship between compressive strength (fc) and tensile strength (ft) for both AC3 and RC3, using high strength values obtained from all samples.

Acknowledgments

We appreciate Sphinx University for their assistance in supplying us with all possible options in the concrete structure laboratory.

References

1109/2002, E. (2002), *Egyptian Standard Specification: Aggregate for Concrete*, Ministry of Industry, Egypt.

Abaqus, S. (2014), *Abaqus/CAE 6.14 User's Manual*, Online Documentation Help: Dassault Systèmes Simulia Corp.

Agwa, I.S., Omar, O.M., Tayeh, B.A. and Abdelsalam, B.A. (2020), "Effects of using rice straw and cotton stalk ashes on the properties of lightweight self-compacting concrete", *Constr. Build. Mater.*, **235**, 117541. https://doi.org/10.1016/j.conbuildmat.2019.117541

Almuwbber, O., Haldenwang, R., Mbasha, W. and Masalova, I. (2018), "The influence of variation in cement characteristics on workability and strength of SCC with fly ash and slag additions", *Constr. Build. Mater.*, **160**, 258-267. https://doi.org/10.1016/j.conbuildmat.2017.11.039

Amin, M. and Tayeh, B.A. (2020), "Investigating the mechanical and microstructure properties of fibre-reinforced lightweight concrete under elevated temperatures", *Case Stud. Constr. Mater.*, **13**, e00459. https://doi.org/10.1016/j.cscm.2020.e00459

Amran, Y.M., Farzadnia, N. and Ali, A.A. (2015), "Properties and applications of foamed concrete; a review", *Constr. Build. Mater.*, **101**, 990-1005. https://doi.org/10.1016/j.conbuildmat.2015.10.112

Astm, C. (2004), "231, Standard Test Method for Air Content of Freshly Mixed Concrete by the Pressure Method", *Annual Book of ASTM Standards*, **4**.

B 212-99, A.B.o.A.S. (2001), *Standard Test Method for Determination of Apparent Density of FreeFlowing Metal Powders Using the Hall Flowmeter Funnel*, ASTM, ASTM.

Batayneh, M., Marie, I. and Asi, I. (2007), "Use of selected waste materials in concrete mixes", *Waste Manage.*, **27**(12), 1870-1876. https://doi.org/10.1016/j.wasman.2006.07.026

Bentz, D.P. and Stutzman, P.E. (1994), "Evolution of porosity and calcium hydroxide in laboratory concretes containing silica fume", *Cement Concr. Res.*, **24**(6), 1044-1050. https://doi.org/10.1016/0008-8846(94)90027-2

Chen, B. and Liu, J. (2008), "Experimental application of mineral admixtures in lightweight concrete with high strength and workability", *Constr. Build. Mater.*, **22**(6), 1108-1113. https://doi.org/10.1016/j.conbuildmat.2007.03.001

Chen, H.J., Tsai, W.P., Tang, C.W. and Liu, T.H. (2011), "Time-dependent properties of lightweight concrete using sedimentary lightweight aggregate and its application in prestressed concrete beams", *Adv. Mater. Res.*, **168**, 2235-2240. https://doi.org/10.4028/www.scientific.net/AMR.168-170.2235

Chen, W.F., Han, D.J. and Han, D.J. (2007), *Plasticity for Structural Engineers*, J. Ross Publishing.

Citek, D., Rehacek, S., Pavlik, Z., Kolisko, J., Dobias, D. and Pavlikova, M. (2018), "Application of Glass Fiber Waste Polypropylene Aggregate in Lightweight Concrete–thermal properties", *IOP Conference Series: Materials Science and Engineering*, **324**(1), 012025. https://doi.org/10.1088/1757-899X/324/1/012025

Committee, A. (2014), *Guide for Structural Lightweight-Aggregate Concrete-ACI Committee 213*, American Concrete Institute.

Concreate, A. (2017), "Standard specification for lightweight aggregates for structural concrete", *ASTM International*.

Domagala, L. (2020), "Durability of structural lightweight concrete with sintered fly ash aggregate", *Materials*, **13**(20), 4565. https://doi.org/10.3390/ma13204565

E.S.S.4756-1/2009 (2009), *Portland Cement, Ordinary and Rapid Hardening. Egyptian Standard Specification E.S.S. 4756-1*, Ministry of Industry, Egypt.

ECP-203, E. (2007), *Egyptian Code for Design and Construction of Reinforced Concrete Structures*, Housing and Building National Research Center, Ministry of Housing, Utilities and Urban Planning, Cairo, Egypt.
Fahmy, M.F. and Idriss, L.K. (2019), "Flexural behavior of large scale semi-precast reinforced concrete T-beams made of natural and recycled aggregate concrete", *Eng. Struct.*, **198**, 109525. https://doi.org/10.1016/j.engstruct.2019.109525
Funnel, H. (1999), "Standard test method for apparent density of free-flowing metal powders using the hall flowmeter funnel", *ASTM Int*, **2**, 89-91.
Gamal, Y.A. and Abd Elrazek, M. (2022), "Evaluation of the seismic performance of lightweight concrete multistory buildings", *IOP Conference Series: Materials Science and Engineering*, **1269**(1), 012004
Guglielmi, P., Silva, W., Repette, W. and Hotza, D. (2010), "Porosity and mechanical strength of an autoclaved clayey cellular concrete", *Adv. Civil Eng.*, **2010**. https://doi.org/10.1155/2010/194102
Haido, J.H., Zainalabdeen, M.A. and Tayeh, B.A. (2021), "Experimental and numerical studies on flexural behavior of high strength concrete beams containing waste glass", *Adv. Concr. Constr.*, **11**(3), 239. https://doi.org/10.12989/acc.2021.11.3.239
Hamada, H., Alattar, A., Yahaya, F., Muthusamy, K. and Tayeh, B.A. (2021), "Mechanical properties of semi-lightweight concrete containing nano-palm oil clinker powder", *Phys. Chem. Earth, Parts a/b/c*, **121**, 102977. https://doi.org/10.1016/j.pce.2021.102977
Hamada, H.M., Al-Attar, A.A., Tayeh, B. and Yahaya, F.B.M. (2022), "Optimizing the concrete strength of lightweight concrete containing nano palm oil fuel ash and palm oil clinker using response surface method", *Case Stud. Constr. Mater.*, **16**, e01061. https://doi.org/10.1016/j.cscm.2022.e01061
Hilal, A.A., Thom, N.H. and Dawson, A.R. (2016), "Failure mechanism of foamed concrete made with/ without additives and lightweight aggregate", *J. Adv. Concr. Technol.*, **14**(9), 511-520. https://doi.org/10.3151/jact.14.511
Hussein, Y.M., Abd Elrahman, M., Elsakhawy, Y., Tayeh, B.A. and Tahwia, A.M. (2022), "Development and performance of sustainable structural lightweight concrete containing waste clay bricks", *J. Mater. Res. Technol.*, **21**, 4344-4359. https://doi.org/10.1016/j.jmrt.2022.11.042
Ibrahim, O.M.O. and Tayeh, B.A. (2020), "Combined effect of lightweight fine aggregate and micro rubber ash on the properties of cement mortar", *Adv. Concr. Constr.*, **10**(6), 537-546. https://doi.org/10.12989/acc.2020.10.6.537
Idriss, L.K. and Gamal, Y.A.S. (2022), "Properties of rubberized concrete prepared from different cement types", *Recycling*, **7**(3), 39. https://doi.org/10.3390/recycling7030039
INSTITUTE, A.C. (2014), *ACI 213R-14: Guide for Structural Lightweight-Aggregate Concrete*, Farmington Hills.
Jankowiak, T. and Lodygowski, T. (2005), "Identification of parameters of concrete damage plasticity constitutive model", *Found. Civil Environ. Eng.*, **6**(1), 53-69.
Joohari, I., Ishak, N.F. and Amin, N.M. (2018), "Mechanical Properties of Lightweight Concrete Using Recycled Cement-Sand Brick as Coarse Aggregates Replacement", *E3S Web of Conferences*, **34**, 01029. https://doi.org/10.1051/e3sconf/20183401029
Kabir, M.I., Lee, C., Rana, M.M. and Zhang, Y. (2020), "Flexural behaviour of ECC-LWC encased slender high strength steel composite beams", *J. Constr. Steel Res.*, **173**, 106253. https://doi.org/10.1016/j.jcsr.2020.106253
Kalyana Rama, J., Chauhan, D., Sivakumar, M., Vasan, A. and Murthy, A.R. (2017), "Fracture properties of concrete using damaged plasticity model-A parametric study", *Struct. Eng. Mech.*, **64**(1), 59-69. https://doi.org/10.12989/sem.2017.64.1.059
Kim, H.K., Jeon, J. and Lee, H.K. (2012), "Workability, and mechanical, acoustic and thermal properties of lightweight aggregate concrete with a high volume of entrained air", *Constr. Build. Mater.*, **29**, 193-200. https://doi.org/10.1016/j.conbuildmat.2011.08.067
Kunchariyakun, K., Asavapisit, S. and Sombatsompop, K. (2015), "Properties of autoclaved aerated concrete incorporating rice husk ash as partial replacement for fine aggregate", *Cement Concr. Compos.*, **55**, 11-16. https://doi.org/10.1016/j.cemconcomp.2014.07.021
Lee, Y.L., Tan, C.S., Lim, S.K., Mohammad, S. and Lim, J.H. (2018), "Strength performance on different mix

of cement-sand ratio and sand condition for lightweight foamed concrete", *E3S Web of Conferences*, **65**, 02006. https://doi.org/10.1051/e3sconf/20186502006

Lian, C., Zhuge, Y. and Beecham, S. (2011), "The relationship between porosity and strength for porous concrete", *Constr. Build. Mater.*, **25**(11), 4294-4298. https://doi.org/10.1016/j.conbuildmat.2011.05.005

Liu, H., Elchalakani, M., Karrech, A., Yehia, S. and Yang, B. (2021), "High strength flowable lightweight concrete incorporating low C3A cement, silica fume, stalite and macro-polyfelin polymer fibres", *Constr. Build. Mater.*, **281**, 122410. https://doi.org/10.1016/j.conbuildmat.2021.122410

Majhi, R.K., Patel, S.K. and Nayak, A.N. (2021), "Sustainable structural lightweight concrete utilizing high-volume fly ash cenosphere", *Adv. Concr. Constr.*, **12**(3), 257. https://doi.org/10.12989/acc.2021.12.3.257

Mohamed, A.M., Tayeh, B.A., Aisheh, Y.I.A. and Salih, M.N.A. (2023), "Exploring the performance of steel fiber reinforced lightweight concrete: A case study review", *Case Stud. Constr. Mater.*, **18**, e01968. https://doi.org/10.1016/j.cscm.2023.e01968

Narattha, C., Thongsanitgarn, P. and Chaipanich, A. (2015), "Thermogravimetry analysis, compressive strength and thermal conductivity tests of non-autoclaved aerated Portland cement–fly ash–silica fume concrete", *J. Therm. Anal. Calorim.*, **122**(1), 11-20. https://doi.org/10.1007/s10973-015-4724-8

Nukah, P.D., Abbey, S.J., Booth, C.A. and Nounu, G. (2023), "Development of a Lytag-silica fume based lightweight concrete and corresponding design equation for pure bending", *Case Stud. Constr. Mater.*, **18**, e01970. https://doi.org/10.1016/j.cscm.2023.e01970

Owais, M. and Idriss, L.K. (2024), "Modeling green recycled aggregate concrete using machine learning and variance-based sensitivity analysis", *Constr. Build. Mater.*, **440** 137393. https://doi.org/10.1016/j.conbuildmat.2024.137393

Paikara, R.K. and Gyawali, T.R. (2023), "Influence of aluminum powder content and powder-to-sand ratio on the physical and mechanical properties of aerated lightweight mortar", *Clean. Mater.*, **10**, 100213. https://doi.org/10.1016/j.clema.2023.100213

Parande, A. (2013), "Role of ingredients for high strength and high performance concrete–a review", *Adv. Concr. Constr.*, **1**(2), 151. https://doi.org/10.12989/acc.2013.1.2.151

Park, S.B. and Tia, M. (2004), "An experimental study on the water-purification properties of porous concrete", *Cement Concr. Res.*, **34**(2), 177-184. https://doi.org/10.1016/S0008-8846(03)00223-0

Poon, C.S. and Lam, C.S. (2008), "The effect of aggregate-to-cement ratio and types of aggregates on the properties of pre-cast concrete blocks", *Cement Concr. Compos.*, **30**(4), 283-289. https://doi.org/10.1016/j.cemconcomp.2007.10.005

Posi, P., Thongjapo, P., Thamultree, N., Boontee, P., Kasemsiri, P. and Chindaprasirt, P. (2016), "Pressed lightweight fly ash-OPC geopolymer concrete containing recycled lightweight concrete aggregate", *Constr. Build. Mater.*, **127**, 450-456. https://doi.org/10.1016/j.conbuildmat.2016.09.105

Różycka, A. and Pichór, W. (2016), "Effect of perlite waste addition on the properties of autoclaved aerated concrete", *Constr. Build. Mater.*, **120**, 65-71. https://doi.org/10.1016/j.conbuildmat.2016.05.019

Salain, I. (2021), "Effect of water/cement and aggregate/cement ratios on consistency and compressive strength of concrete using volcanic stone waste as aggregates", *Civil Eng. Architect.*, **9**(6), 1900-1908. https://doi.org/10.13189/cea.2021.090621

Şeker, B.Ş., Gökçe, M. and Toklu, K. (2022), "Investigation of the effect of silica fume and synthetic foam additive on cell structure in ultra-low density foam concrete", *Case Stud. Constr. Mater.*, **16**, e01062. https://doi.org/10.1016/j.cscm.2022.e01062

Shabbar, R., Alasadi, L. and Taher, J.K. (2024), "Influence of silica fume addition on enhancing the autoclaved aerated concrete properties", *Magaz. Civil Eng.*, **128**(4), 12808-12808. https://doi.org/10.34910/MCE.128.8

Standard, A. (2014), "C138/C138M–14", *Stand. Test Method Density (Unit Weight. Yield, Air Content Concr. ASTM Int. West Conshohocken, PA*.

Tanyildizi, H. and Coskun, A. (2008), "Performance of lightweight concrete with silica fume after high temperature", *Constr. Build. Mater.*, **22**(10), 2124-2129. https://doi.org/10.1016/j.conbuildmat.2007.07.017

Tawfik, T.A., AlSaffar, D.M., Tayeh, B.A., Metwally, K.A. and ElKattan, I.M. (2021), "Role of expanded clay aggregate, metakaolin and silica fume on the of modified lightweight concrete properties", *Geosyst.*

Eng., **24**(3), 145-156. https://doi.org/10.1080/12269328.2021.1887002
Tayeh, B.A., Hakamy, A., Amin, M., Zeyad, A.M. and Agwa, I.S. (2022), "Effect of air agent on mechanical properties and microstructure of lightweight geopolymer concrete under high temperature", *Case Stud. Constr. Mater.*, **16**, e00951. https://doi.org/10.1016/j.cscm.2022.e00951
Tayeh, B.A., Zeyad, A.M., Agwa, I.S. and Amin, M. (2021), "Effect of elevated temperatures on mechanical properties of lightweight geopolymer concrete", *Case Stud. Constr. Mater.*, **15**, e00673. https://doi.org/10.1016/j.cscm.2021.e00673
Vakhshouri, B. (2020), "Structural lightweight concrete containing expanded poly-styrene beads; Engineering properties", *Steel Compos. Struct.*, **34**(4), 581-597. https://doi.org/10.12989/scs.2020.34.4.581
Vakhshouri, B. and Nejadi, S. (2016), "Self-compacting light-weight concrete; mix design and proportions", *Struct. Eng. Mech.*, **58**(1), 143-161. https://doi.org/10.12989/sem.2016.58.1.143
Van, L.T., Kim, D.V., Xuan, H.N., Dinh, T.V., Bulgakov, B. and Bazhenova, S. (2019), "Effect of aluminium powder on light-weight aerated concrete properties", *E3S Web of Conferences*, **97**, 02005. https://doi.org/10.1051/e3sconf/20199702005
Verma, S.K. and Ashish, D.K. (2017), "Mechanical behavior of concrete comprising successively recycled concrete aggregates", *Adv. Concr. Constr.*, **5**(4), 303. https://doi.org/10.12989/acc.2017.5.4.303
Wang, J., Zheng, K., Cui, N., Cheng, X., Ren, K., Hou, P., Feng, L., Zhou, Z. and Xie, N. (2020), "Green and durable lightweight aggregate concrete: The role of waste and recycled materials", *Materials*, **13**(13), 3041. https://doi.org/10.3390/ma13133041
Wee, T.H., Babu, D.S., Tamilselvan, T. and Lim, H.S. (2006), "Air-void system of foamed concrete and its effect on mechanical properties", *ACI Mater. J.*, **103**(1), 45.
Youssf, O., Hassanli, R., Elchalakani, M., Mills, J.E., Tayeh, B.A. and Agwaa, I.S. (2023), "Punching shear behaviour and repair efficiency of reinforced eco-friendly lightweight concrete slabs", *Eng. Struct.*, **281**, 115805. https://doi.org/10.1016/j.engstruct.2023.115805
Yu, T., Teng, J., Wong, Y. and Dong, S. (2010), "Finite element modeling of confined concrete-I: Drucker–Prager type plasticity model", *Eng. Struct.*, **32**(3), 665-679. https://doi.org/10.1016/j.engstruct.2009.11.014
Yun, T.S., Jeong, Y.J., Han, T.S. and Youm, K.S. (2013), "Evaluation of thermal conductivity for thermally insulated concretes", *Energy Build.*, **61**, 125-132. https://doi.org/10.1016/j.enbuild.2013.01.043
Zhao, H., Sun, W., Wu, X. and Gao, B. (2015), "The properties of the self-compacting concrete with fly ash and ground granulated blast furnace slag mineral admixtures", *J. Clean. Prod.*, **95**, 66-74. https://doi.org/10.1016/j.jclepro.2015.02.050

CC